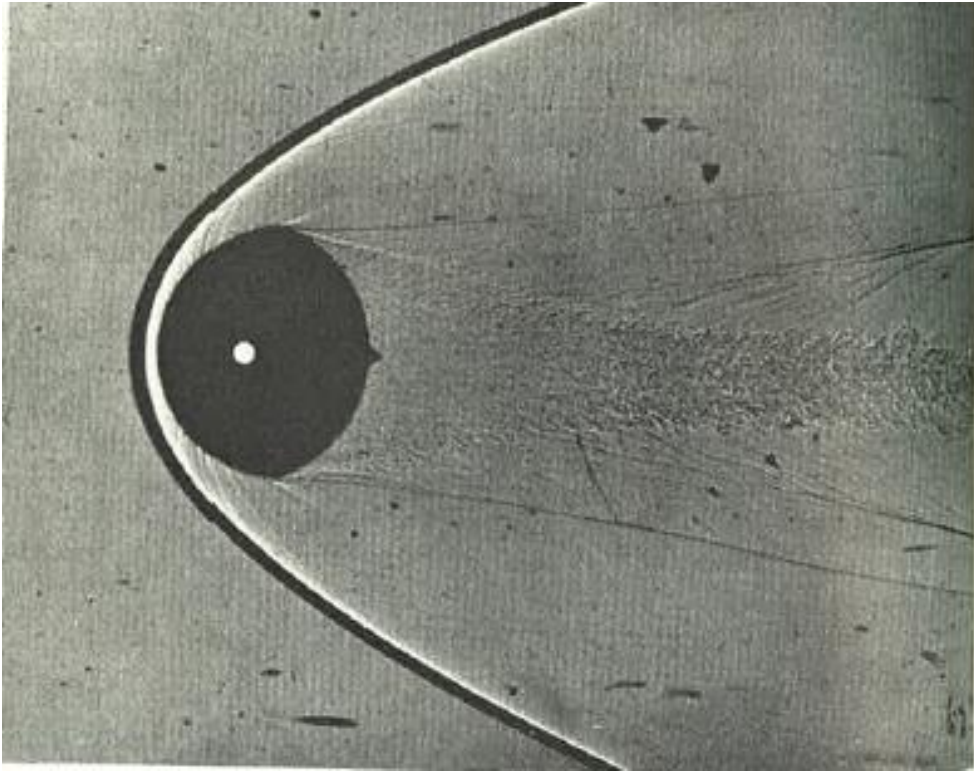


International Space Sciences School
Heliospheric physical processes for understanding Solar
Terrestrial Relations
21-26 September 2015

George K. Parks,
Space Sciences Laboratory, UC Berkeley, Berkeley, CA

**Lecture 3: Earth's Bow Shock and
Foreshock Dynamics**



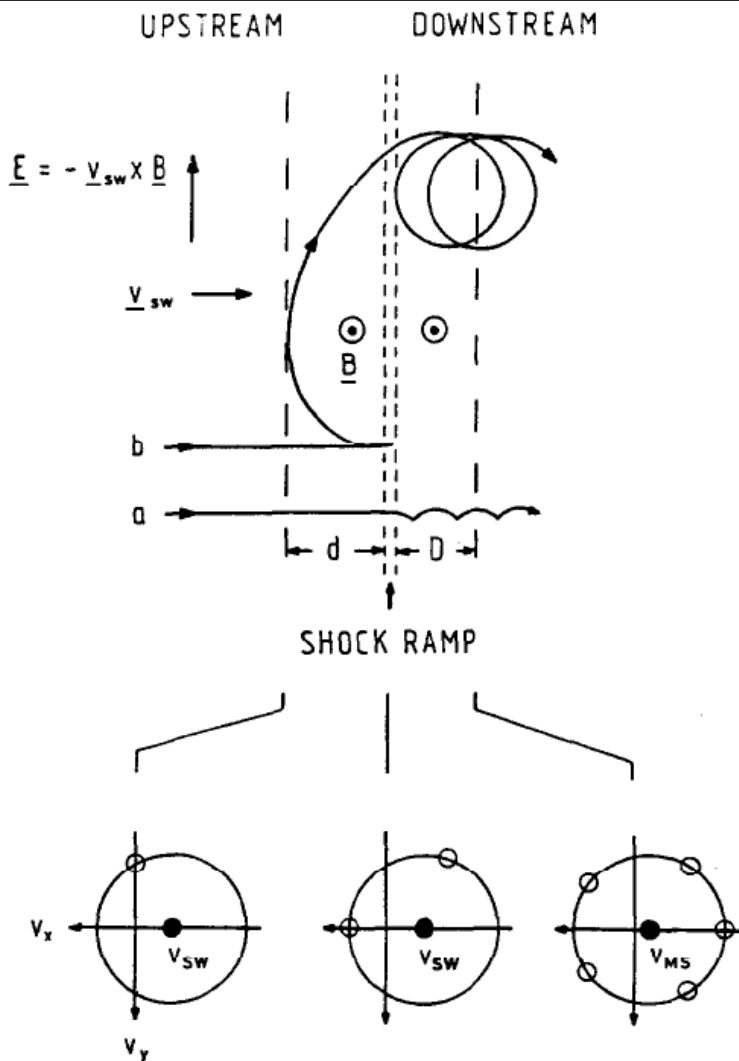
- A fluid picture of the bow shock is based on the magnetosphere launching a magnetosonic wave which interacts with the supersonic SW steepening into a standing shock wave.
- The supersonic SW flow thermalizes and the downstream plasma consists of *subsonic* hotter thermalized SW.
- However, observations show the bow shock is much more complicated than the fluid shock.

Introduction

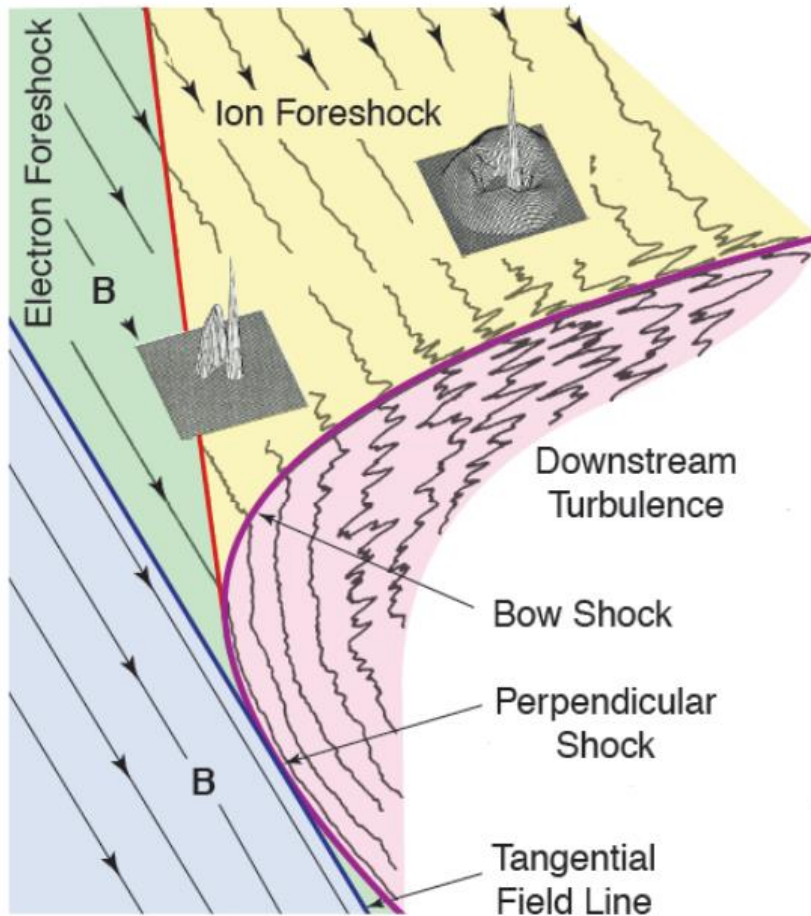
- T. Gold introduced the concept of collisionless shock in 1955 to explain fast rise time of sudden commencements (SCs).
- This idea received much attention from fusion researchers interested in heating plasma to high temperatures and astrophysicists seeking ways to accelerate particles to cosmic energies.
- Serious debates followed about what mechanisms could *thermalize* and produce *entropy* without collisions.
- The debates ended without a clear resolution of theoretical issues when *super-Alfvenic* solar wind was discovered.
- The magnetic discontinuity in front of Earth (bow shock) was accepted as evidence of a collisionless shock.

Introduction (cont'd)

- The width of Earth's bow shock is about ion Larmor radius, ~ 7 orders of magnitude smaller than the SW collision mean free path $\lambda_c \sim 1$ AU.
- This challenged theorists to look at collisionless shock in new ways, but physical mechanisms of how the SW dissipate energy and generate entropy on scales of ion Larmor radius remains unclear to this day.
- Bow shock is very different from ordinary shocks. For example, 20% of incident SW is *reflected*. The 80% of *transmitted SW* does not thermalize immediately (Sckopke, 1990; 1995).
- Many years of bow shock observations have shown thermalization and entropy generation mechanisms involve integrated dynamics *upstream* and *downstream* of the shock, and *at the transition* region.

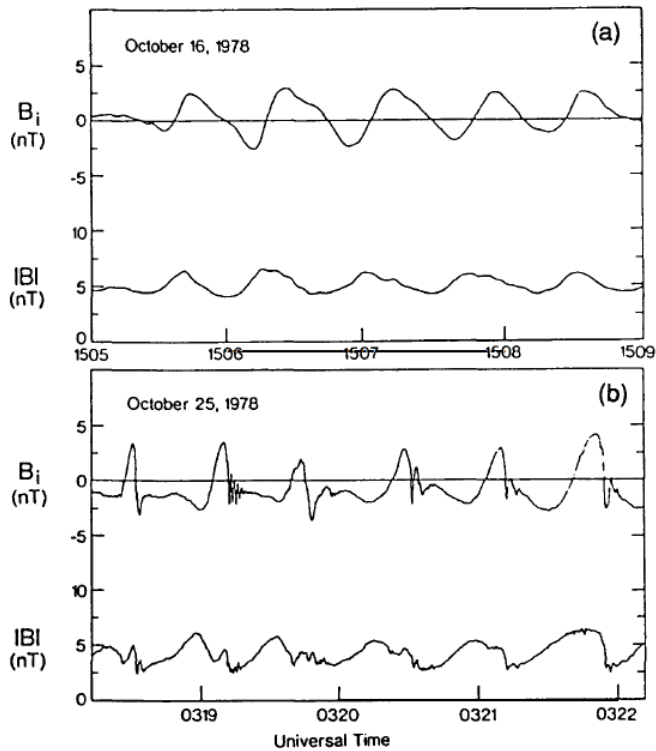


- Bow shock is *different* from ordinary shocks: up to 20% of SW is reflected while the remaining 80% is directly transmitted across the shock.
- Reflected ions are accelerated by the SW electric field and gyrate back to the shock.
- Transmitted SW does not immediately thermalize in the MS region. Note beam has been slowed down.
- Bottom: Ion distributions expected at three locations. Incident and directly transmitted (big dots), labeled V_{sw} and V_{MS} . Initial reflected ions (open circles) whose radius is about gyrospeed, $v_g \sim 2 V_{sw}$ (specular reflection).

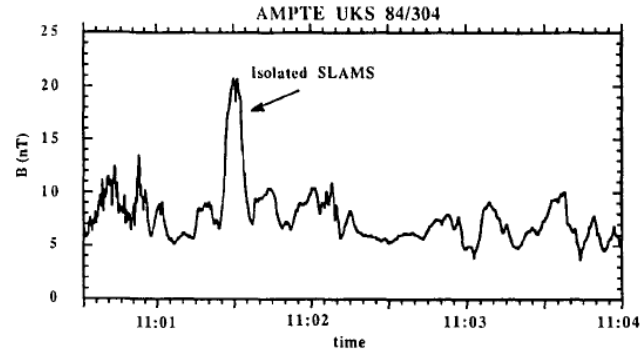


- Bow Shock dynamics depend on θ_{BN}
- θ_{BN} changes direction from dusk to dawn.
- For $\theta_{BN} > 45^\circ$, *quasi-perpendicular region* (dusk sector)
- For $\theta_{BN} < 45^\circ$, *quasi-parallel shock region* (dawn sector).
- Reflected SW particles in the quasi-perpendicular shock region propagate to upstream region and form
 - *Electron foreshock* boundary
 - *Ion foreshock* boundary

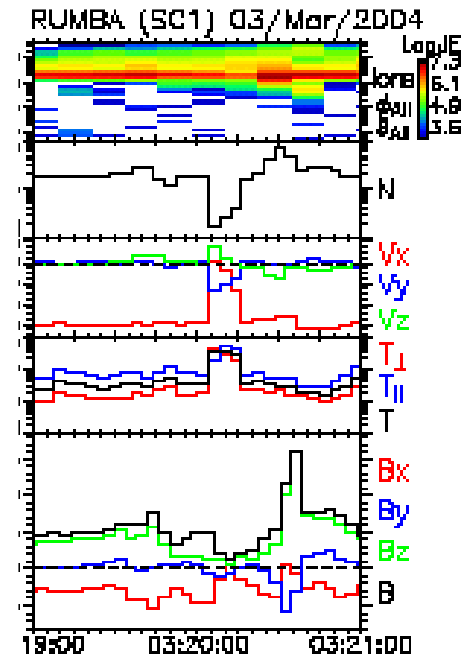
Treumann and Scholer, 2001



Schwartz, 1990



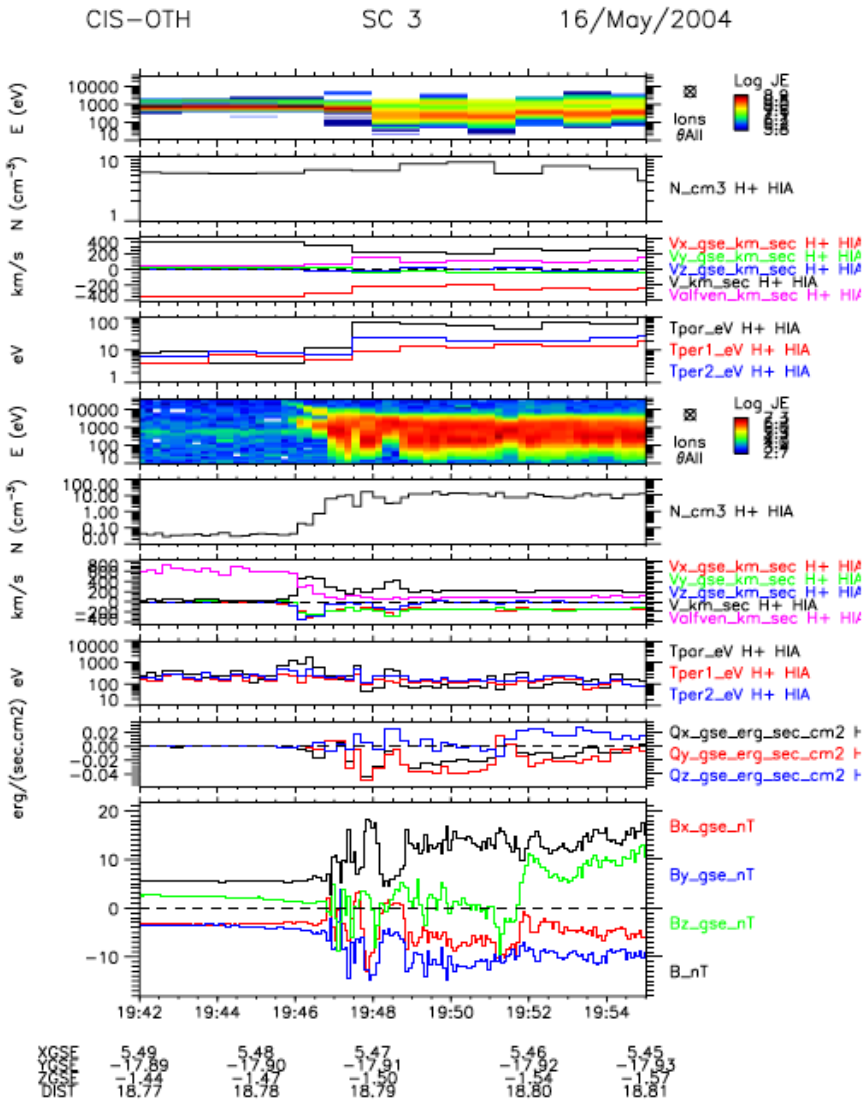
Schwartz, 1990



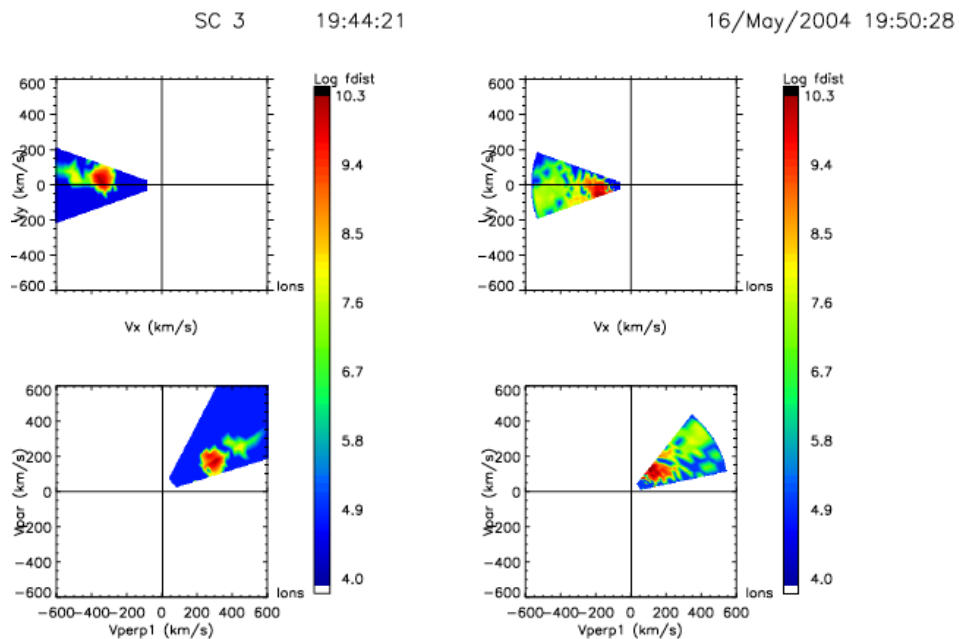
Parks et al, 2006

- Reflected SW interacts with incident SW and produce *transient nonlinear structures* in the upstream region.
- The upstream nonlinear structures subsequently convect with the SW affecting the bow shock structure and dynamics.
- Upstream nonlinear structures are an integral part of the bow shock dynamics.

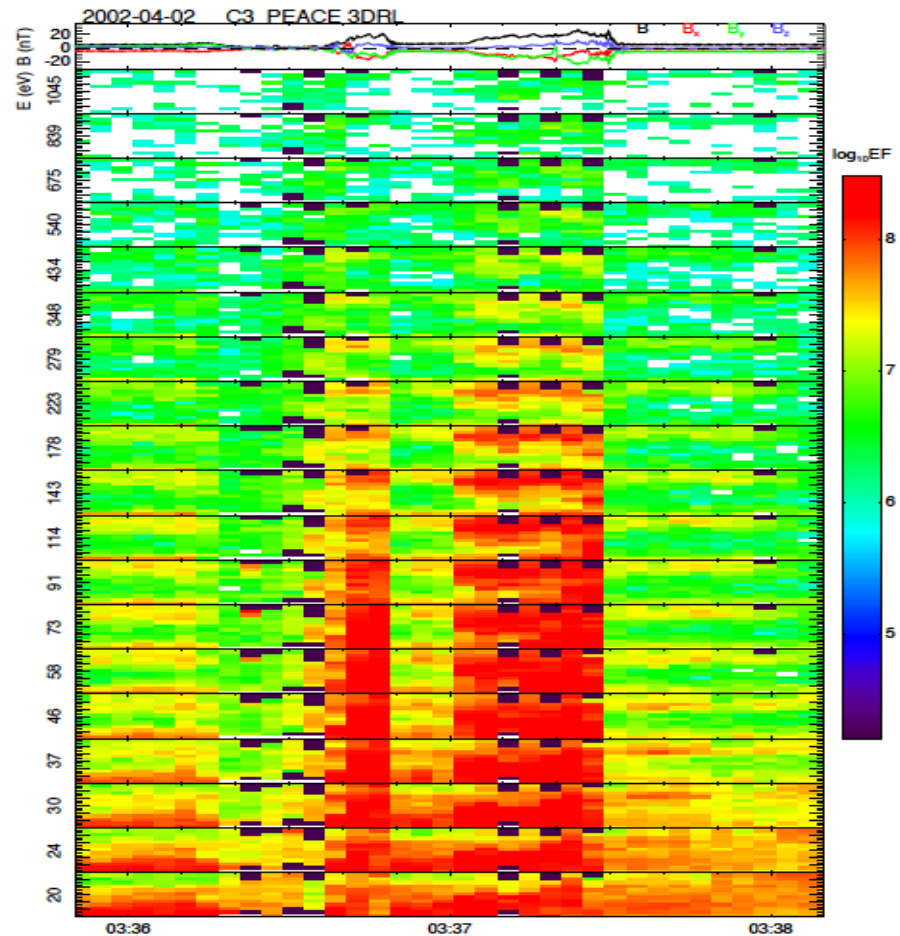
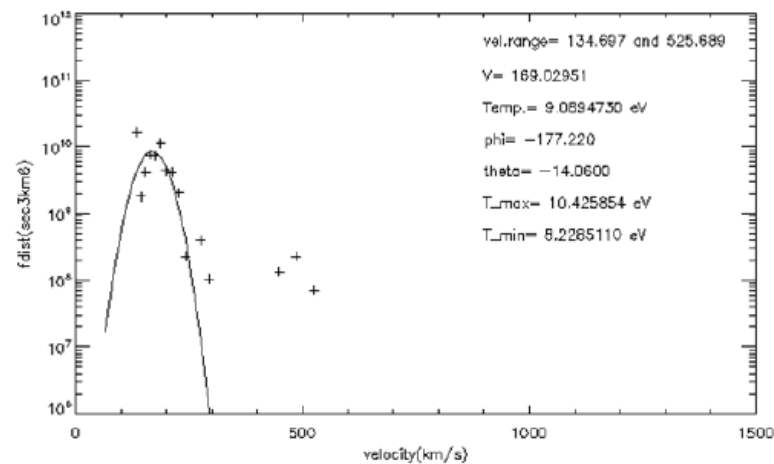
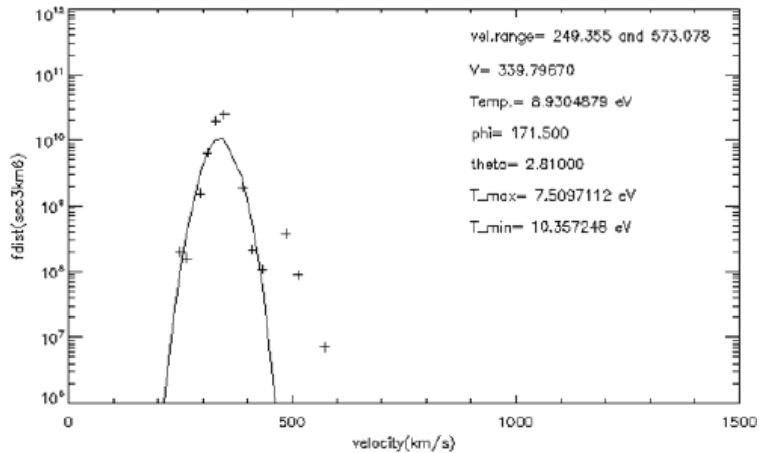
Observations of a typical bow shock



- SW remains super-Alfvenic downstream of bow shock.
- SW beams often penetrate in to the downstream magnetosheath.



Ion beams are slowed down

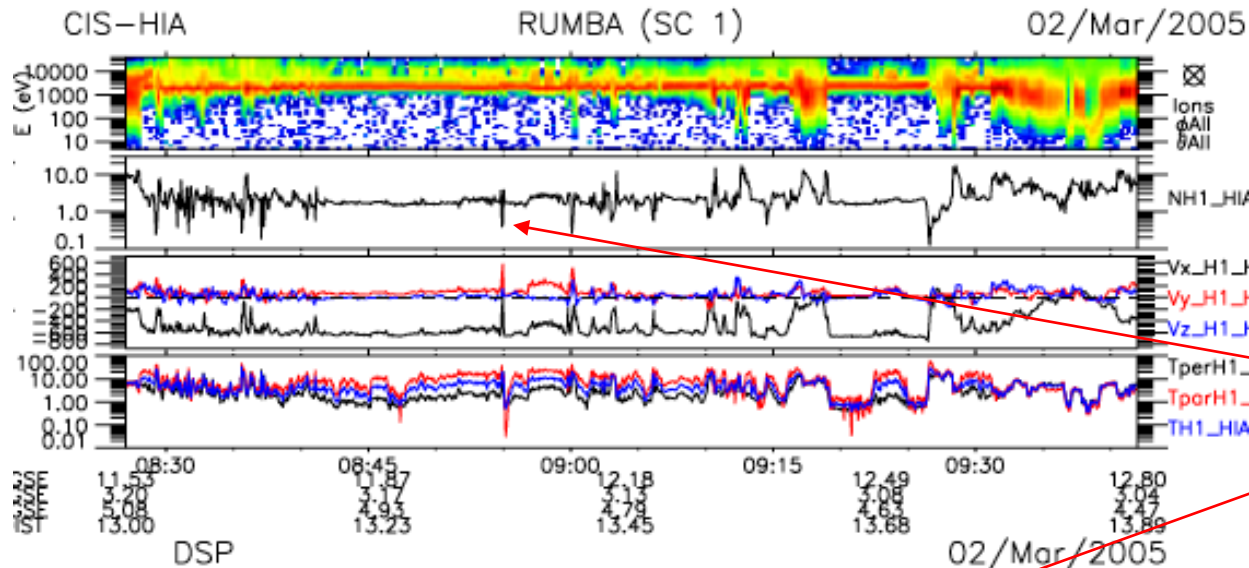


- What slows down the SW beam across the shock?
- Usual explanation is that the bow shock potential decelerates the SW ions.
- However, we see electrons backstreaming (*Caveat*: Don't know if electrons are SW electrons reflected from the bow shock or leakage from Magsheath).

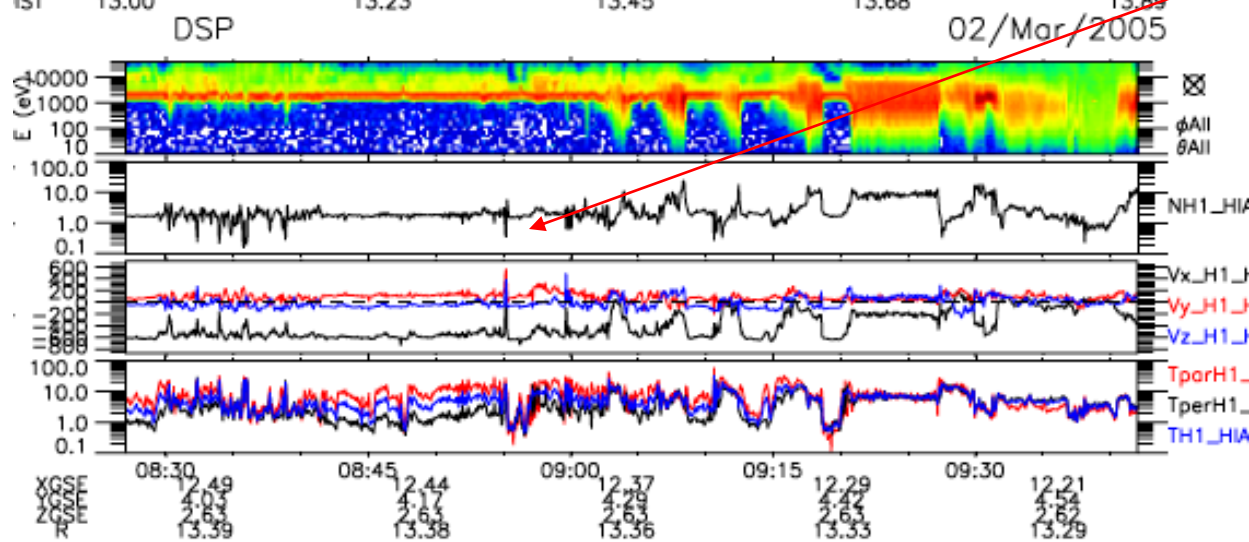
Known Transient disturbances upstream of bow shock

- *Hot flow anomaly (HFA)* (aka Hot Diamagnetic Cavity, HDC): Depressed B field, $\sim R_E$ scale length, filled with hot plasma, flow deflected from the solar wind direction (Schwartz, 1985; Thomsen, 1986) *~ 30 events seen by AMPTE and ISEE.*
- *Short, Large Amplitude Magnetic Structures (SLAMS)*: Enhancement of B at least 2-4 times the solar wind field. Time scale ~ 10 s, length $\sim R_E$. *Occurs frequently.* (Schwartz, 1991; Giacalone, 1993)
- *Foreshock Cavity (FC)*: Diamagnetic cavity filled with slightly hotter plasma than SW and flowing in nearly the same direction as the solar wind (Sibeck, 2002).
- **Density hole**: *Ion Larmor size structure with density depleted at the center and enhanced at the edges. Occurs very frequently* (Parks, 2006).

Density Holes discovered by Cluster and Double Star



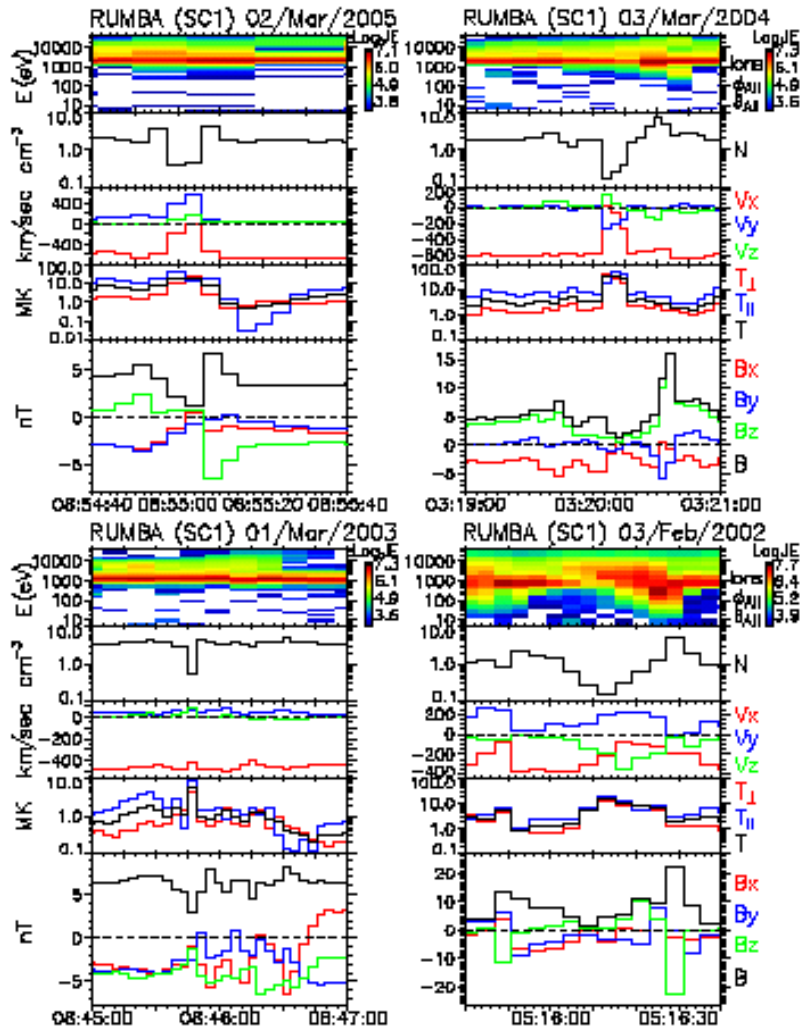
“Spikes” that go above and below SW density levels.



Cluster 4 identical SC.
Orbit plane normal to ecliptic plane.

Double Star
Equator apogee 13.5RE

Examples of Density Holes



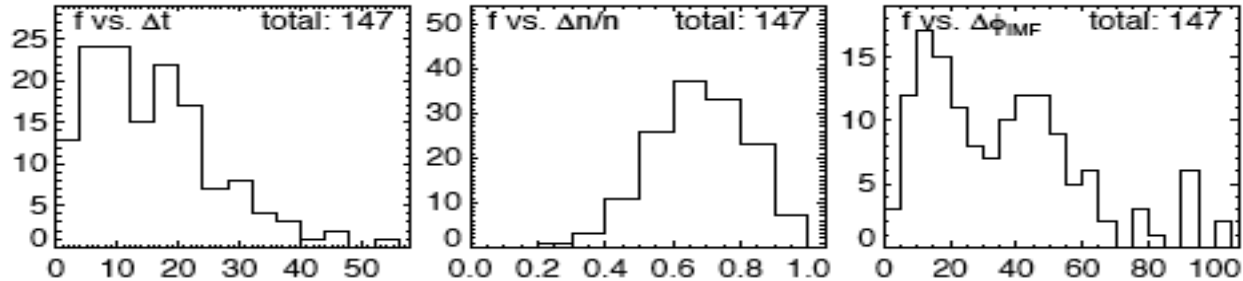
- $\delta n/n$ as large as 0.98
- Duration as short as 4s
- Edges overshoot, $\sim 2-6$ times
- Slowdown of SW: $V_x \sim 0$, V_y, V_z deviated.
- T increases inside ($T > 10^7$ °K)
- Similarly shaped B-holes.
- B generally changes sign in the hole indicating crossing of a *CS*
- *Backstreaming population* necessary for DH

Statistical studies of 147 events

$$\Delta t \sim 18 \pm 10 \text{ s}$$

$$\delta n/n \sim 0.7 \pm 0.14$$

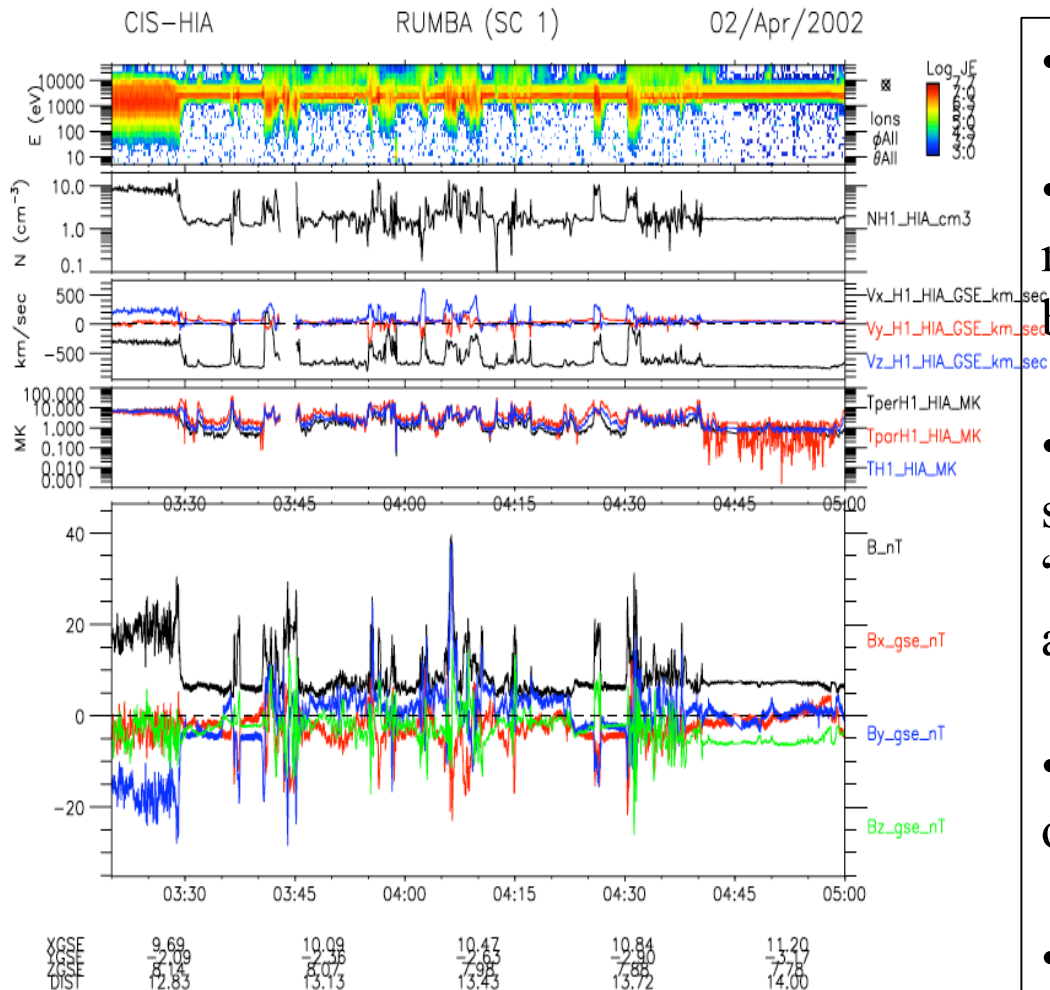
$$36^\circ \pm 24^\circ$$



- **typical ~18s but some as short as 4s**
- **$\delta n/n \sim 0.6-0.94$**
- **Large variation of B and components often sign change**
- **Mean rotation of B $\sim 36^\circ \pm 24^\circ$ (Large error due to 4s data used).**

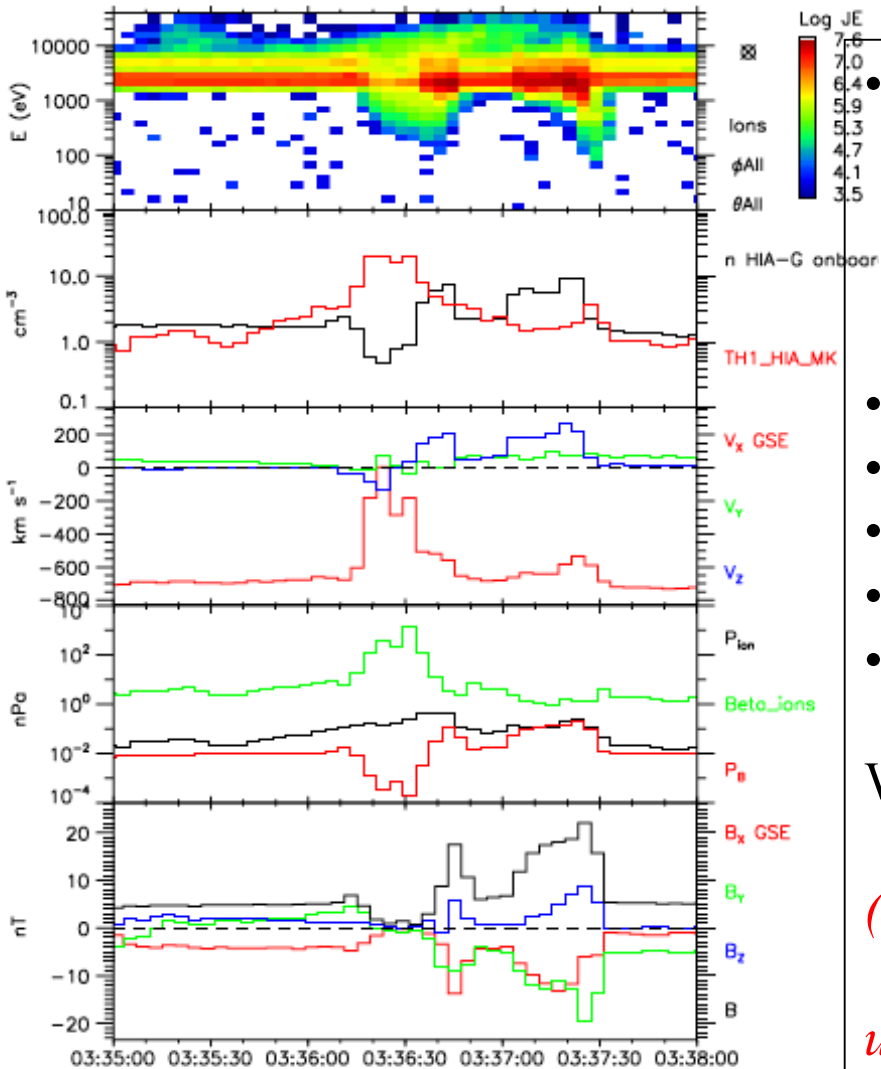
Upstream Structures: Similarities and Differences

	DH	HFA	FC	SLAMS
Duration	~18 s	~few minutes	>few minutes	~10-20 s
Scale length	~R_G	~ R_E	>few R_E	~ R_E
$\delta n/n$	~0.7	< 0.2	< 0.2	No report
Bulk V	$V_x \rightarrow \sim 0$	$V_x \rightarrow -100$	~ V_{sw}	No report
T (hole)	~ 10^{6-7}	~ 10^6	> 10^5	No report
Overshoot	Yes	Yes	Yes	Yes
Occurrence	Frequent	Rare	Rare	Frequent
Electron hole	Yes	No report	No report	No report
E-field	Yes	No report	No report	Yes
Waves	Yes	No report	No report	Yes
Shock-like?	Yes	Yes	No	Yes
Backstream ions	Yes	Yes	No report	Inferred
Current J	Yes	No report	No report	Inferred



- Bow shock crossed at ~ 0330 UT
- Typical behavior of plasma and magnetic field upstream of Earth's bow shock.
- On this time scale, nonlinear structures in density appear as “spikes” in density, bulk velocity and magnetic field.
- Some spikes go up and down and others go up or down.
- Large-amplitude magnetic field many times the value of ambient SW magnetic field.

CIS-0TH SC 3 02/Apr/2002



- Two magnetic pulses detected. One remained a steepened magnetic pulse while the other evolved into a nonlinear structure,
- n decreases, T increases, V_x decreases
- $P_{\text{particles}} > P_{\text{magnetic}}$ (*expanding*)
- β inside “hole” reached ~ 1000
- Magnetic field same shape as particles
- By component reverses: presence of CS

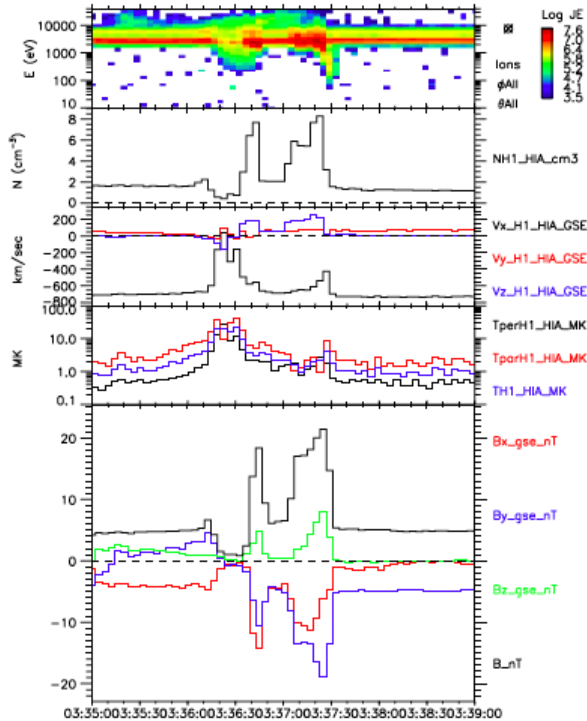
What plasma processes can

(1) select a wave to grow while the neighboring waves remain unchanged?

(2) evolve the magnetic pulsation into a complex nonlinear structure?

XGSE	9.93	9.95	9.96	9.98
YGSE	-2.25	-2.26	-2.27	-2.29
ZGSE	8.08	8.08	8.07	8.07
DIST	13.00	13.01	13.02	13.04

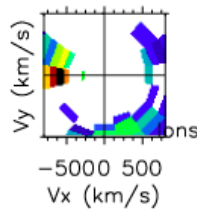
CIS-OTH RUMBA (SC 1) 02/Apr/2002



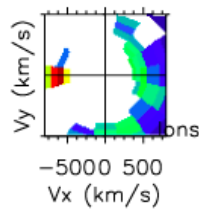
SC	9.93	9.95	9.96	9.98	10.00
UT	13.01	13.02	13.04	13.05	13.06

What causes the SW slow down?

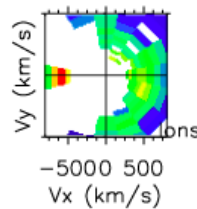
- SW: $V_x \sim 0$ at 0336:22 UT (minimum n)
- However, SW beam is still present.
- SW beam velocity remains constant, *615-645 km/s*.
- SW beam intensity decreases inside density depleted region.



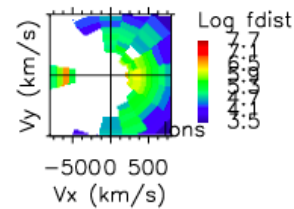
0336:12



0336:16

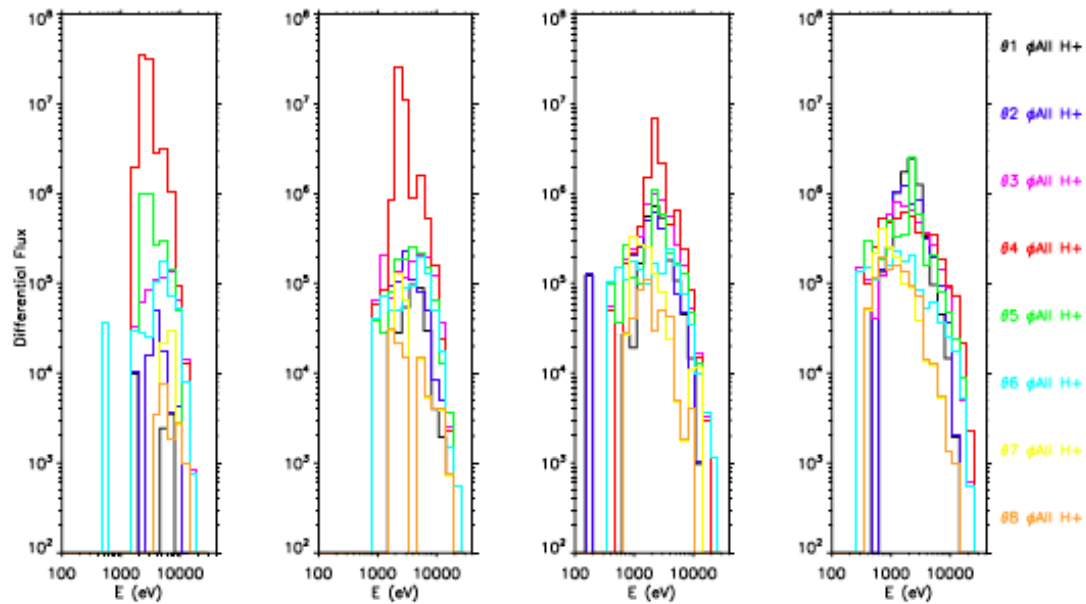
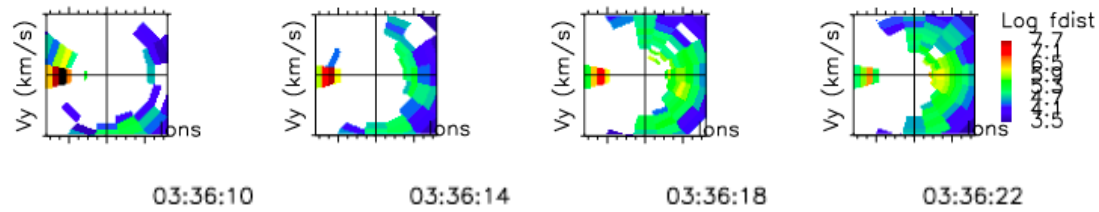


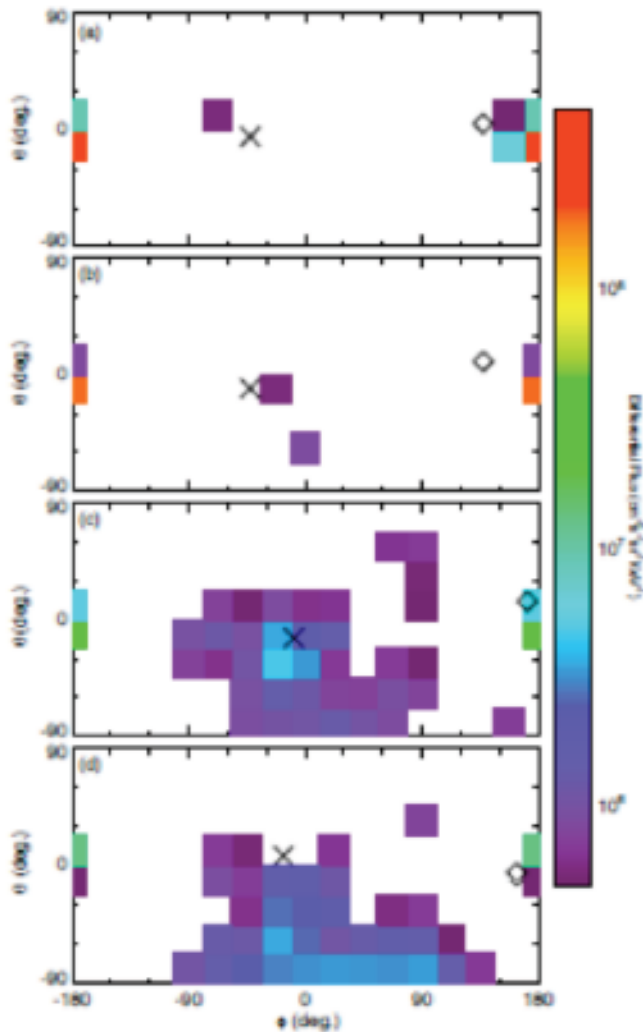
0336:20



0336:22

Intensity of the SW beam is reduced.





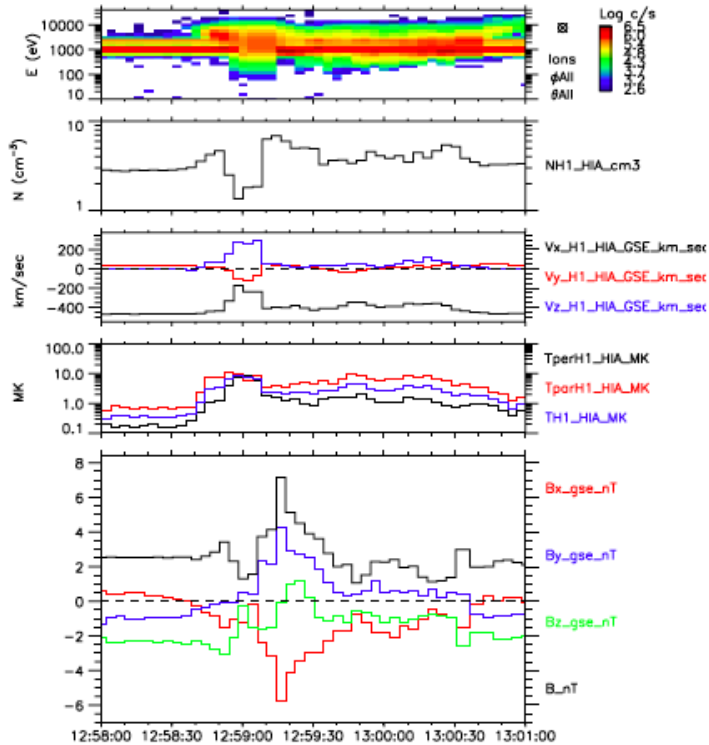
- θ - ϕ plots of the four plots that correspond to the top row for θ and ϕ panels that contain the SW beam.
- There are 8 bins on the Y-axis and 16 on the X-axis. Each panel is separated by 4s.

• SW Bulk velocity $\langle \mathbf{v} \rangle = \int \mathbf{v} f(\mathbf{r}, \mathbf{v}, t) d^3v$ decreases because particles from other directions are *acting against the SW*, thereby *reducing the velocity moment*.

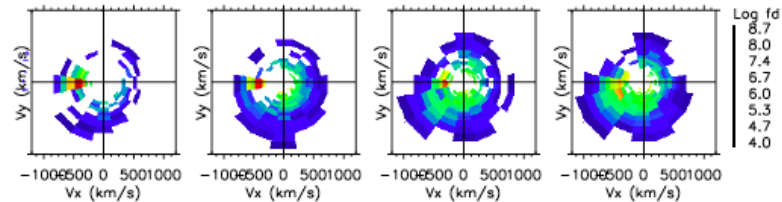
see Parks et al., 2013

Another Example

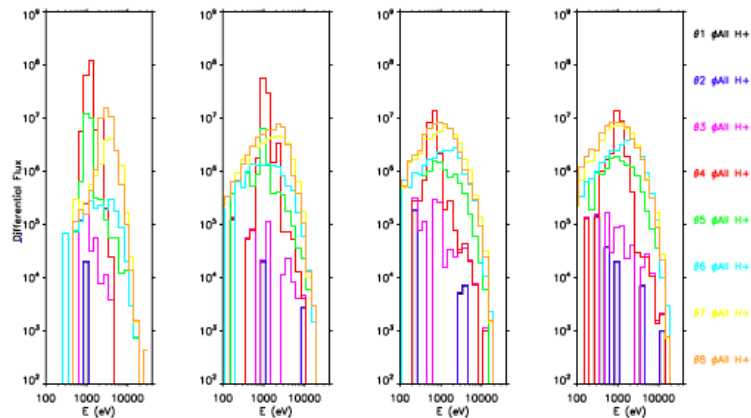
CIS-OTH RUMBA (SC 1) 24/Mar/2001

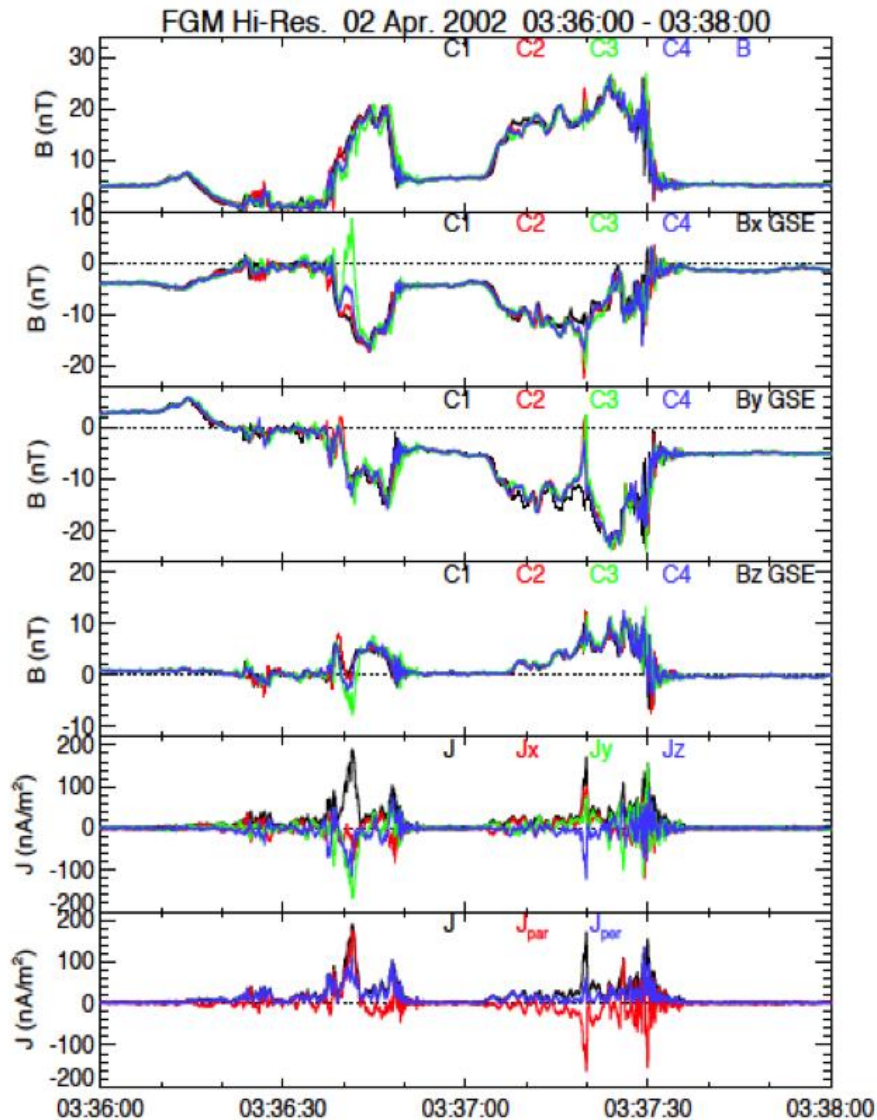


XGSE	8.48	8.49	8.51	8.53
YGSE	0.26	0.25	0.24	0.24
ZGSE	9.06	9.06	9.06	9.06
DIST	12.41	12.42	12.43	12.45



12:58:50 12:58:54 12:58:58 12:59:02





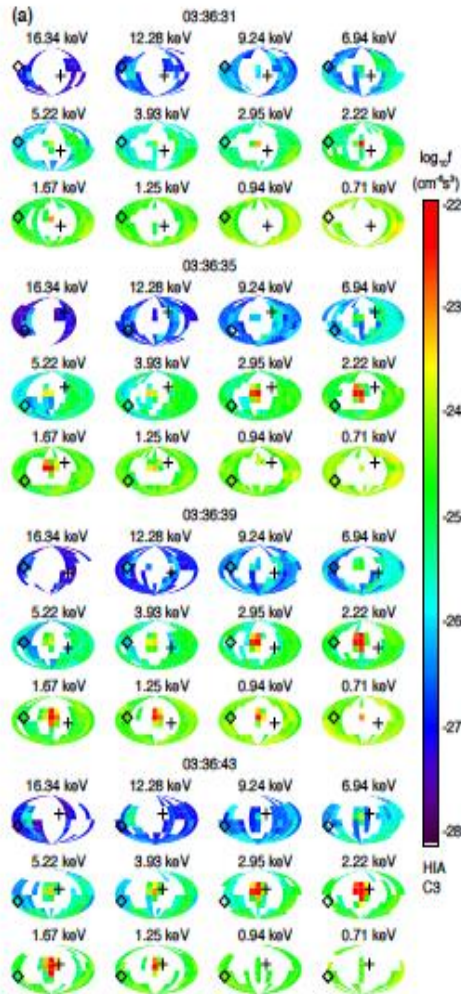
- On 2 April 2002, Cluster operated in *burst mode*. Magnetic field sampled at 67 times/s during the nonlinear structure.

- SC1 (black), SC2 (red), SC3 (green), SC4 (blue)

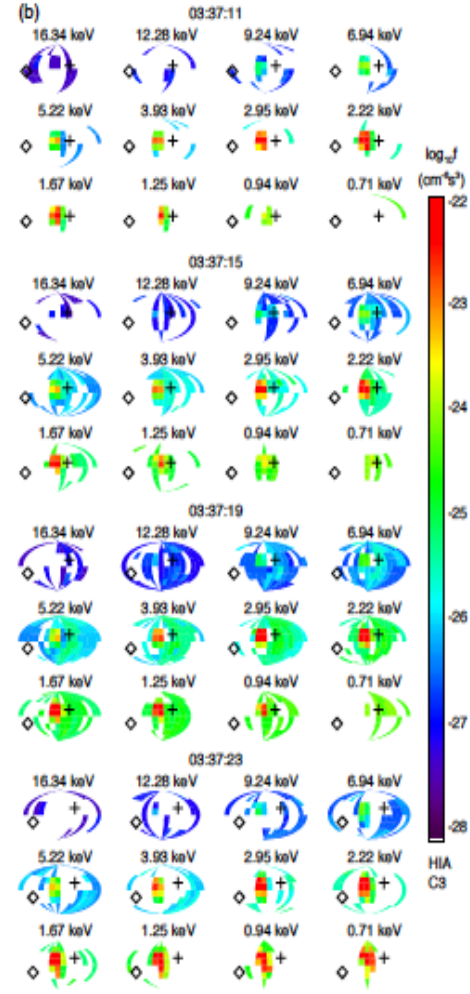
- *Currents* calculated using the “curlometer” method.

- Current densities in directions *parallel* (red) and *perpendicular* (blue) to the magnetic field are in opposite directions for the two events.

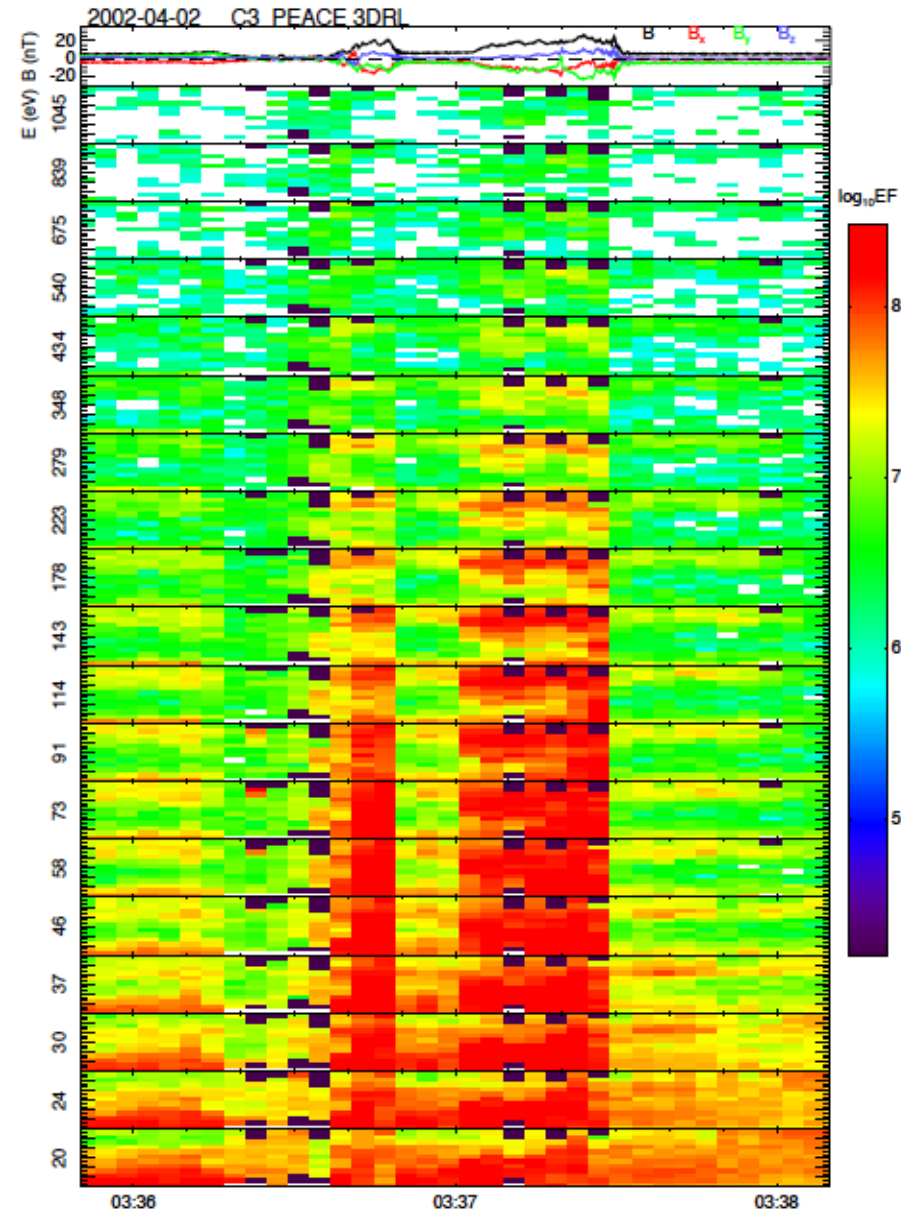
Hammer-Aitoff Plots of 3D Ions (4s)



Beams stream in *both* **B**-directions



Beams stream only along **B**.
No back streaming ions.

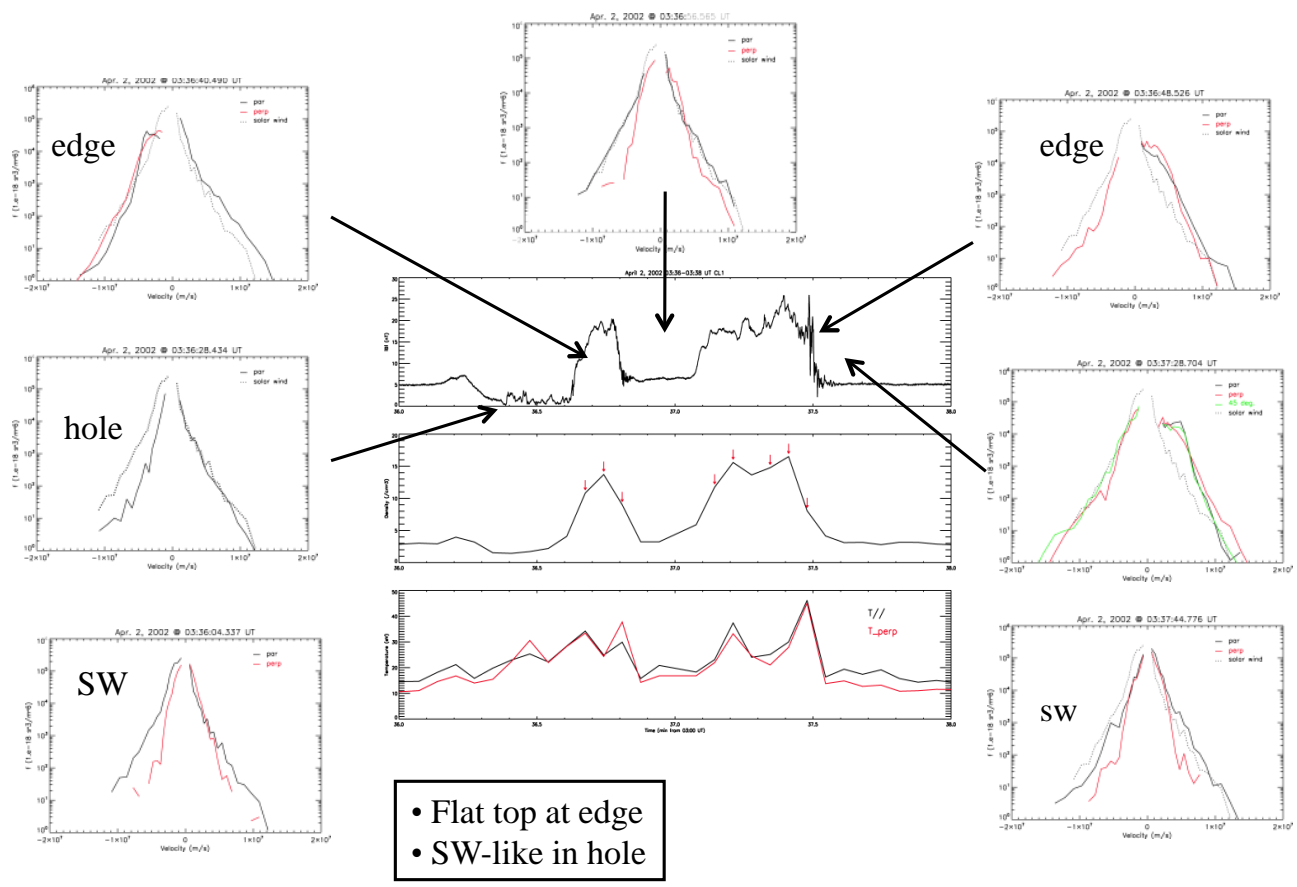


Electron Energy flux spectrogram of electrons measured from 11 eV to 5.5 keV.

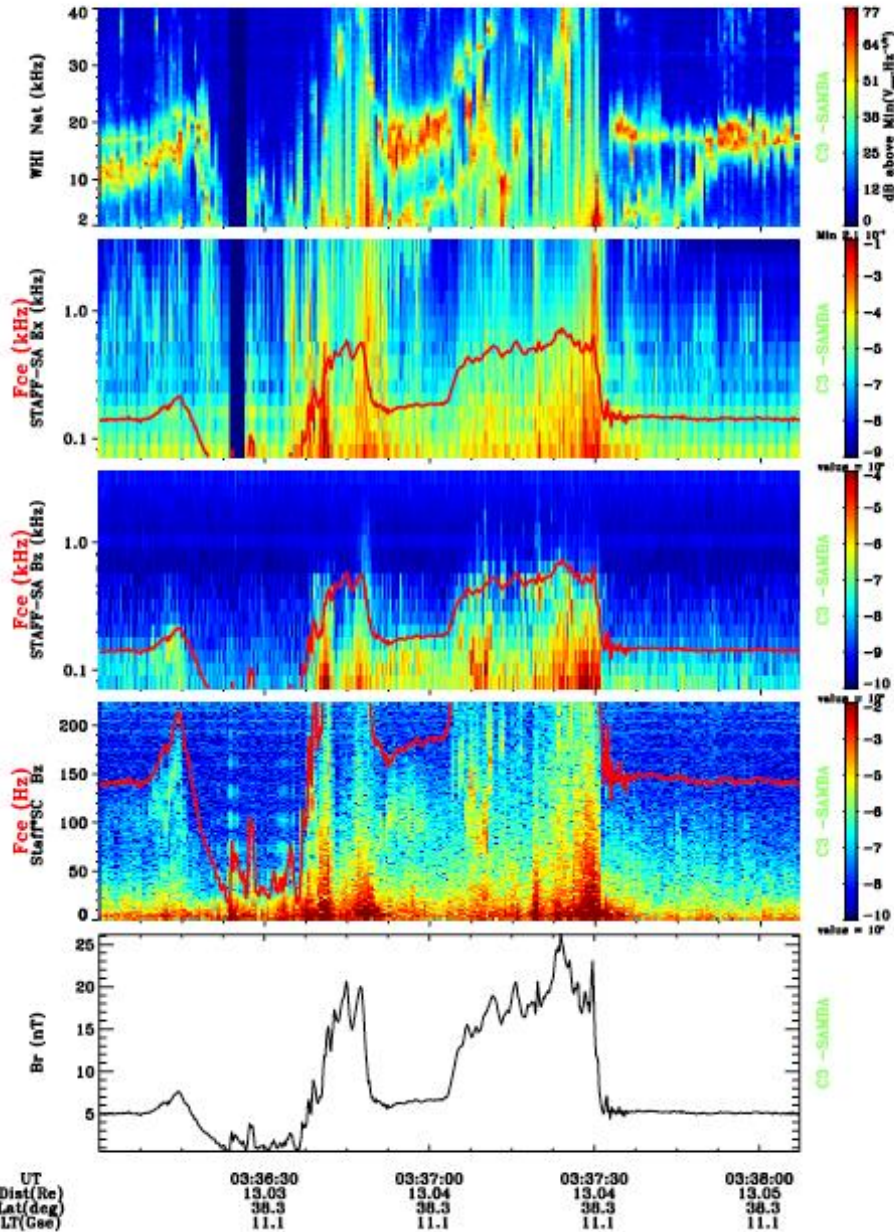
For each energy channel, the Y-axis varies from 0 – 180°.

- 0° electrons at 143 eV are *Strahl electrons*
- 180° electrons reflected, leakage and/or pitch-angle scattered halo and strahl electrons.
- Strahl electrons streaming through field aligned ions form *field-aligned current*.

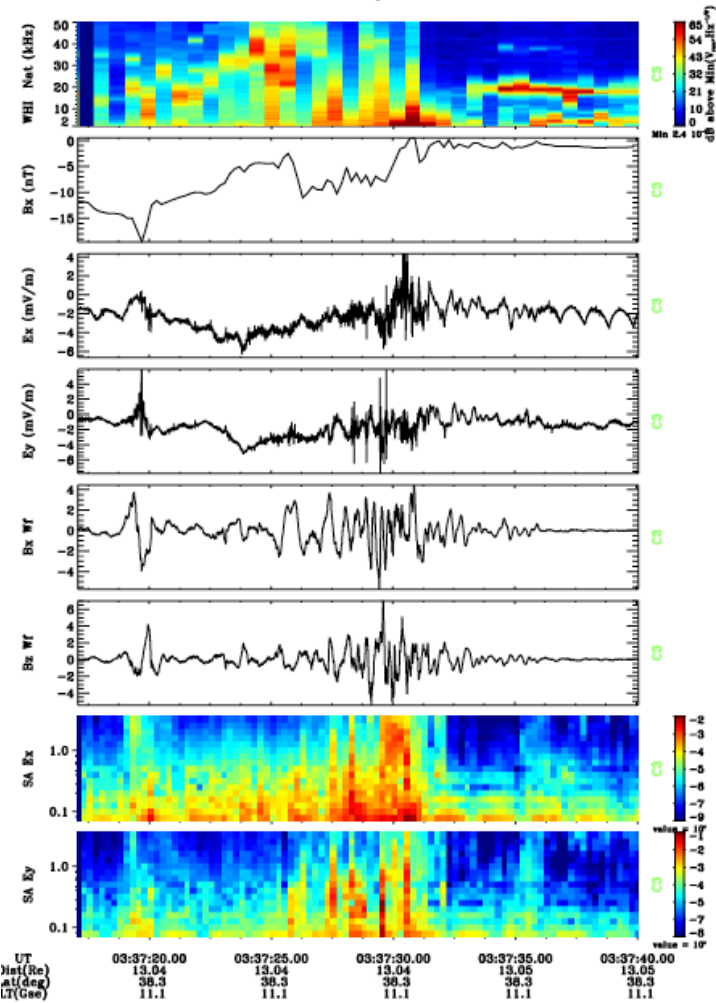
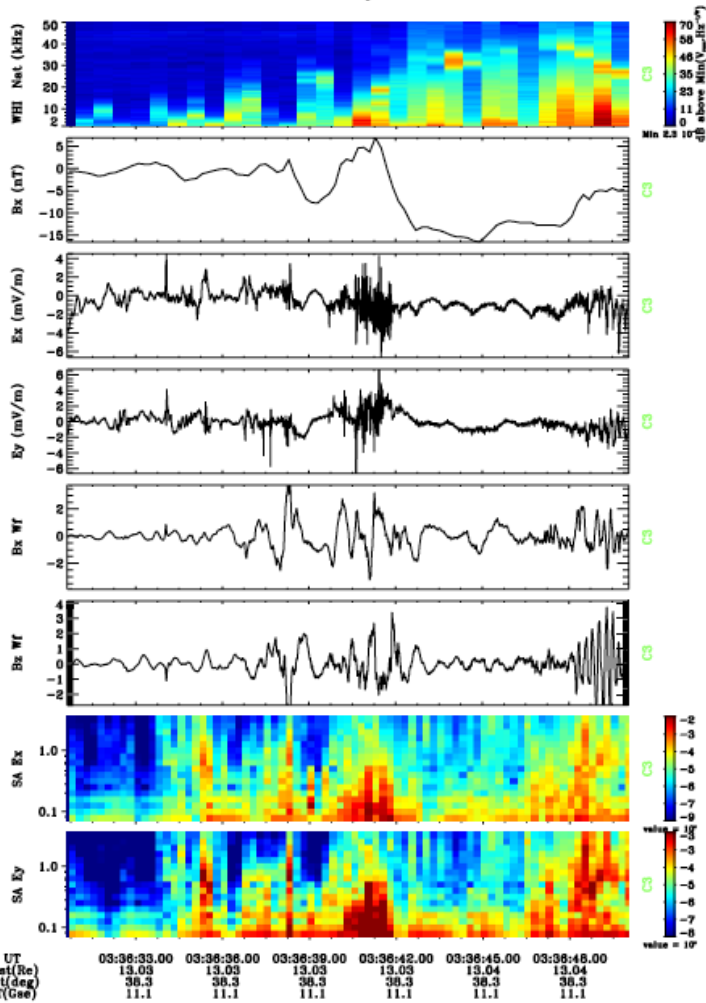
Electron distributions (2 April 02)



Similar flat-top distributions seen at edges of HFAs (Fuselier et al. 1988).

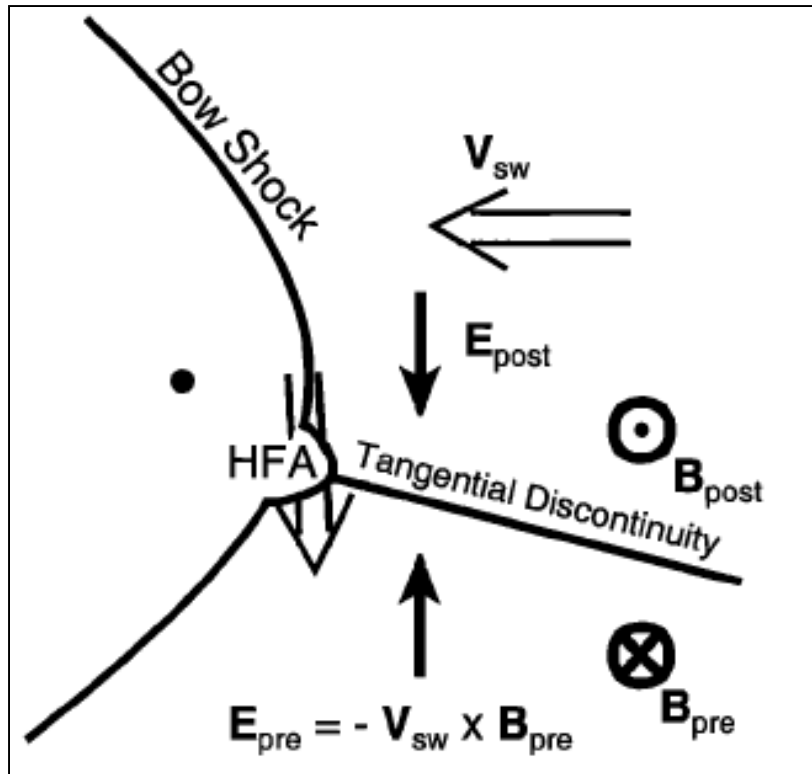


- *Top panel*: ES emissions observed by Whisper (frequency to 40 kHz).
- *Second panel*: electric field component from Staff (64 – 4000 Hz)
- *Third and fourth panels*: magnetic fluctuations, from Staff (64-4000 Hz) and (0.6 to 180 Hz).
- Similar to waves at bow shock (Gurnett, 1985).
- *ES emissions* Broadband observed to plasma frequency.
- Bursty, observed below and above *f_{ce}*, intensifies at both steepened edges.
- ES waves very intense at the first FAC
- Correlated with particle and B variations
- *EM waves* to Fce include whistler mode in front of steepened edges.
- Narrow band EM waves, similar to lion roars in magnetosheath.



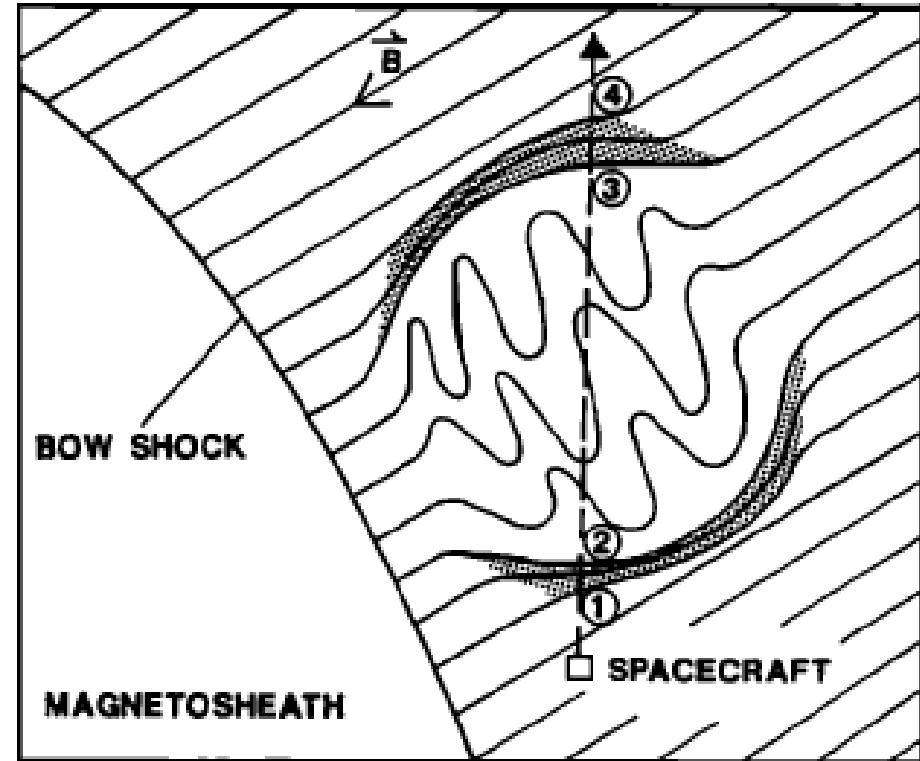
- *EFW spiky*. Spiky bursts can include *Electrostatic Solitary Waves* (Belhke et al., 2004) similar to observations at the bow shock (Matsumoto et al., 1997).
- Time resolution of EFW for the two cases studied is 2.2 ms. Unfortunately, Not adequate to determine if Solitary Waves (<1 ms) were present.

HFA Model: Burgess and Schwartz (1988)



- HFA associated passage of *IMF current sheet* (CS).
- SW E-field points *inward* normal to CS.
- Channels the *reflected particles* into the CS producing a high T region.
- Hot plasma expands
- No Instability

HDC model: Thomsen et al. (1988)

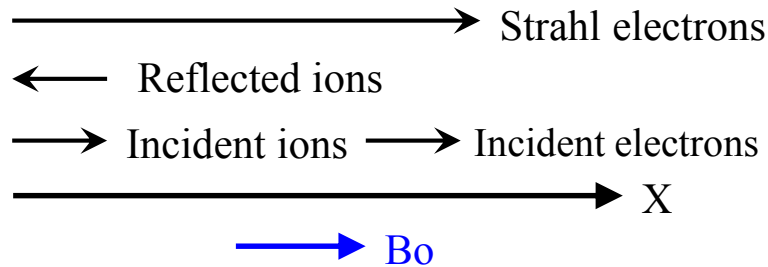


- HDCs due to *large fraction of reflected particles* coupled to SW
- *Ion-ion streaming instability* converts streaming energy to thermal energy
- Hot plasma expands
- Only Ion Dynamics

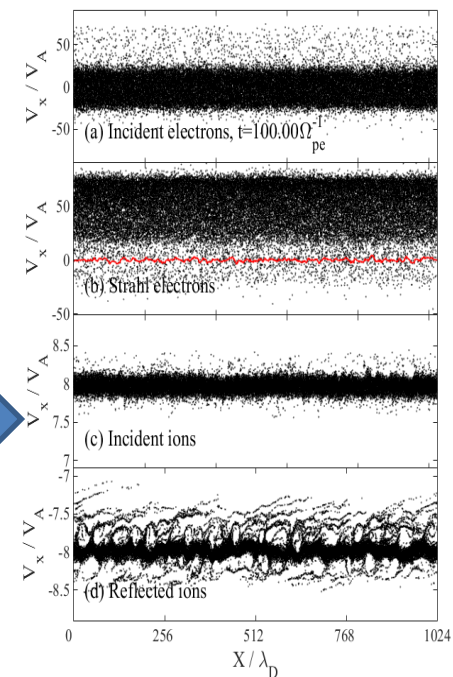
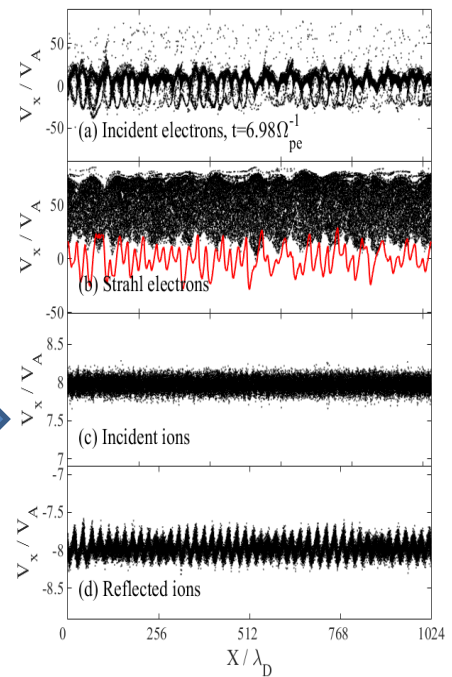
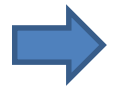
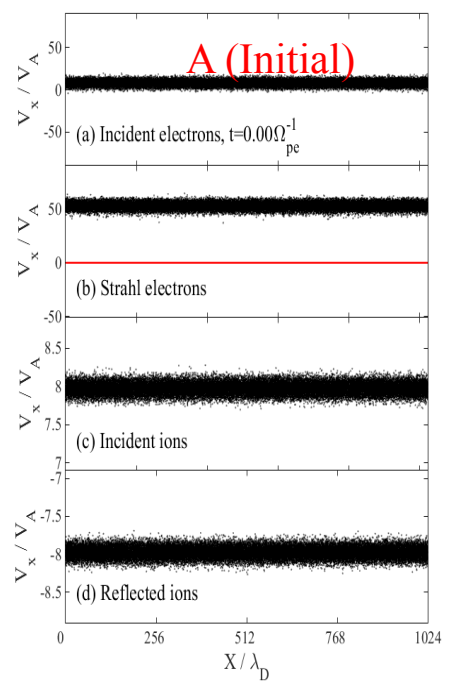
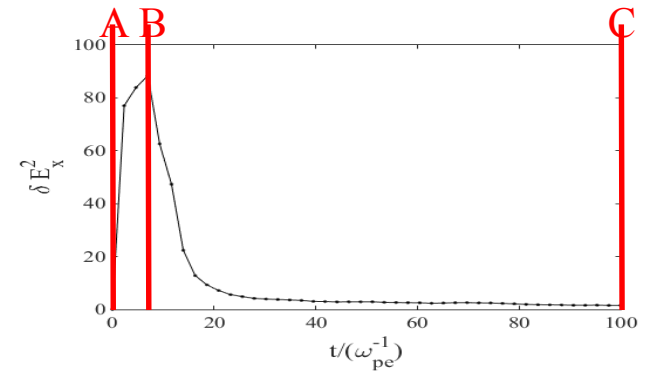
1D Relativistic PIC Simulation code (Dieckmann et al., 2000; Shimada/Hoshino, 2004)

Run 2 (Strahl e^- = 5,
 $\theta_{Bx} = 0^\circ$):

E_x (red)



time-evolution of
 wave energy δE_x^2



Simulation by ZW Yang, CAS, Beijing, China

Step 1: from $t=0$ to $0.006 \Omega_{ci}^{-1}$ (i.e., $11 \Omega_{ce}^{-1}$), everything looks quit.

Step 2: at $t=12.8 \Omega_{ce}^{-1}$, the instability becomes visible (left column). Phase space plots of **strahl electrons** change first.

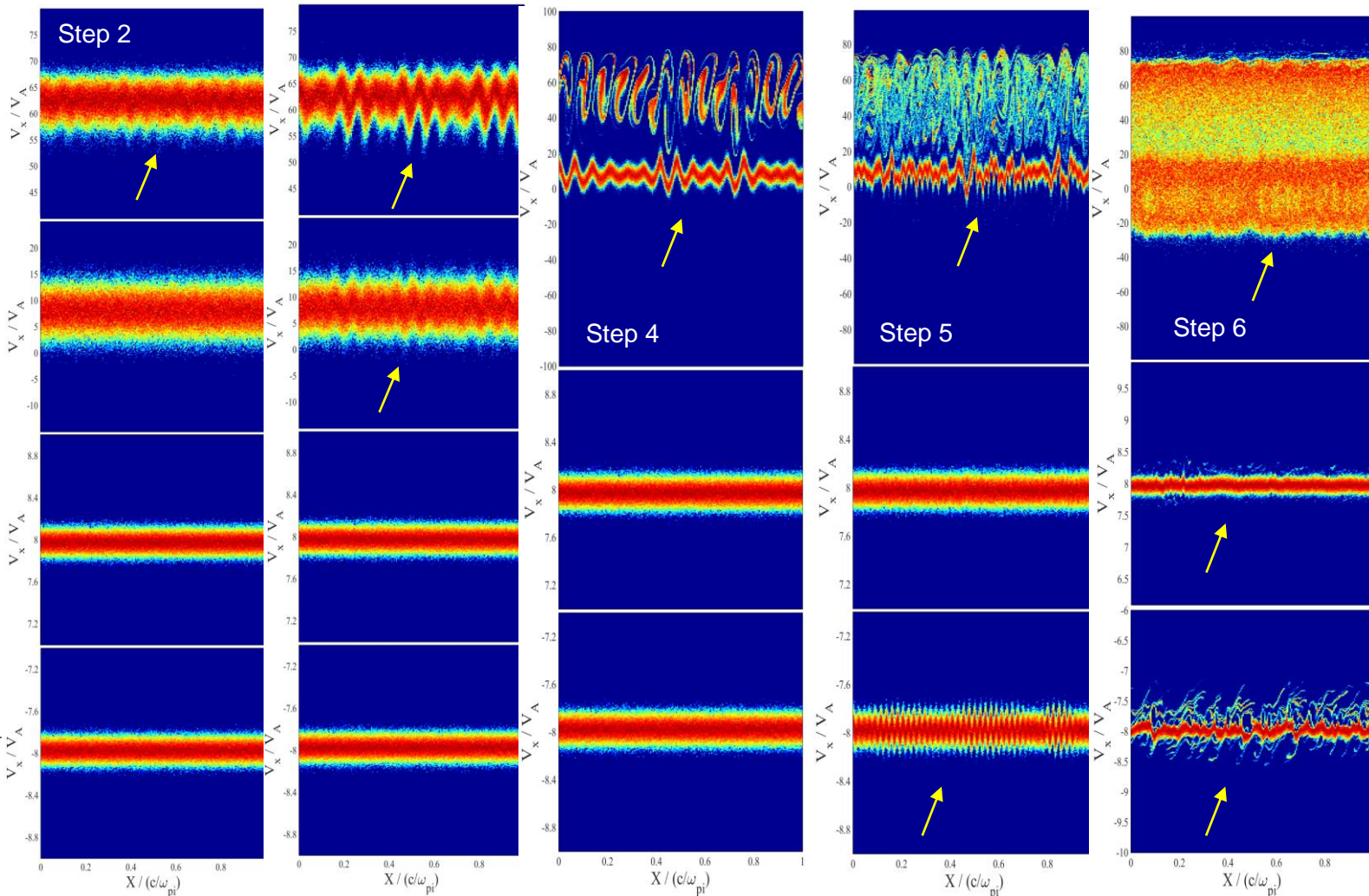
Step 3: at $t=18.3 \Omega_{ce}^{-1}$, **incident electrons** start to couple with strahl electrons.

Step 4: at $t=36.7 \Omega_{ce}^{-1}$, strahl electrons are trapped (phase space hole is visible) by the E_{\parallel} . Ions still have no big change.

Step 5: at $t=73.4 \Omega_{ce}^{-1}$, **reflected ions** begin to couple with electrons in small scale. Electrons are heated.

Step 6: at $t=734 \Omega_{ce}^{-1}$ (i.e., $=0.4 \Omega_{ci}^{-1}$), **incident ions** start to be affected by the E_{\parallel} . Electrons are heated a lot.

(a) strahl e^{-}

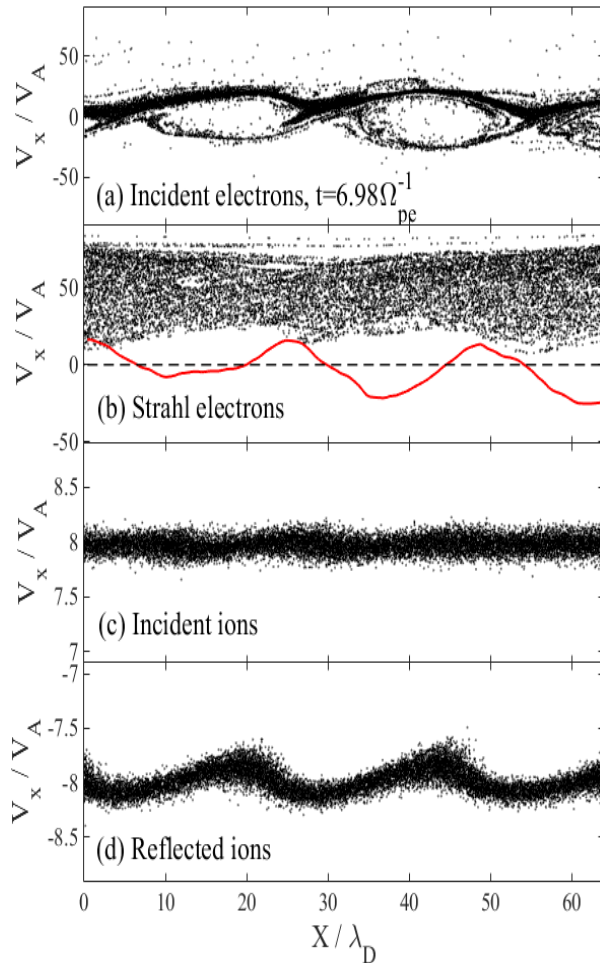


(b) incident e^{-}

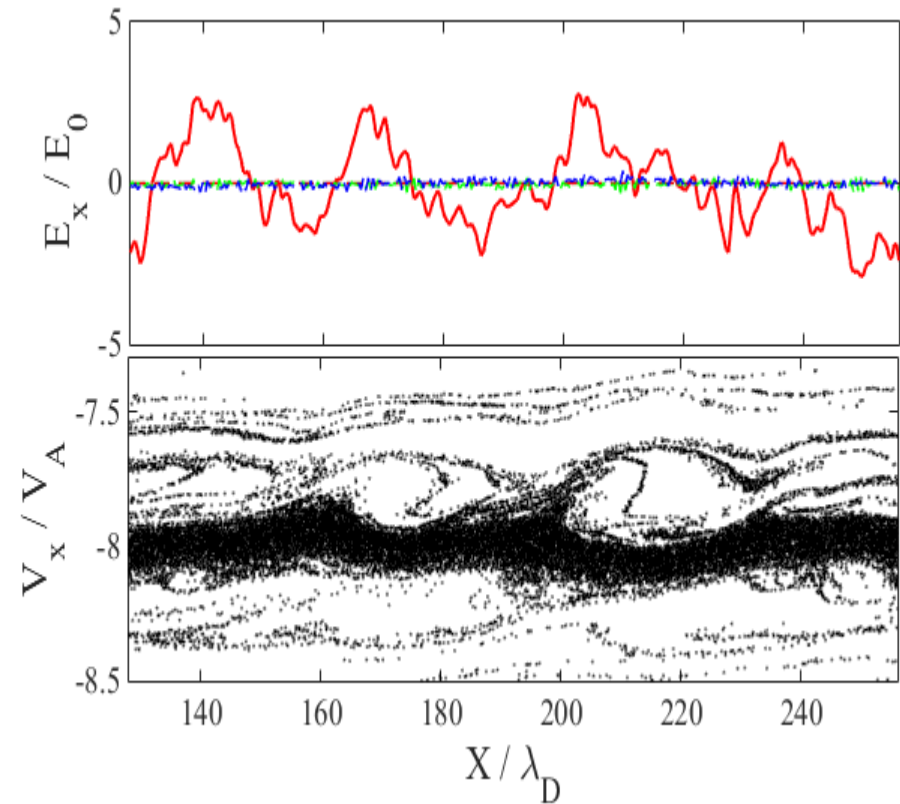
(c) incident H^{+}

(d) reflected He^{++}

B (early)



C (Later)

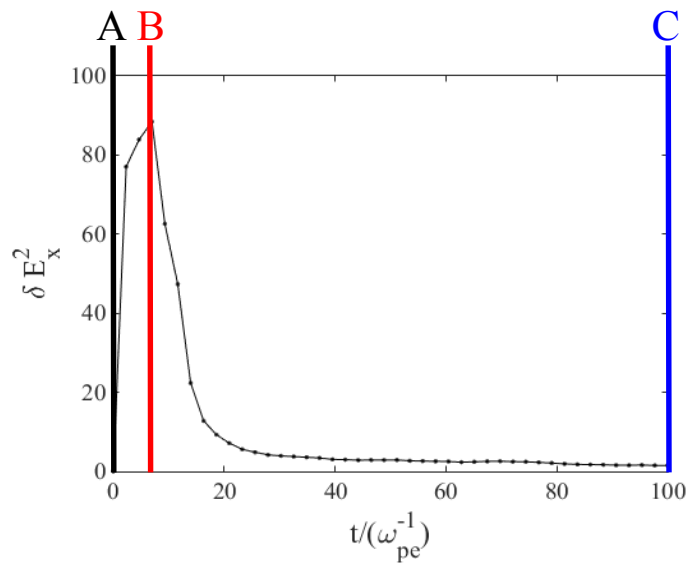


Zoom in: the spikes of the reflected ions are due to the modulation by the bi-polar E_x (*red*) structure which correspond to electron phase space holes.

E_x (*red*) bi-polar structure much weaker than earlier. It leads to density hole of the *reflected ions*. (E_y, E_z, B_y and $B_z \sim 0$ dashed curves, different colors. Top panel).

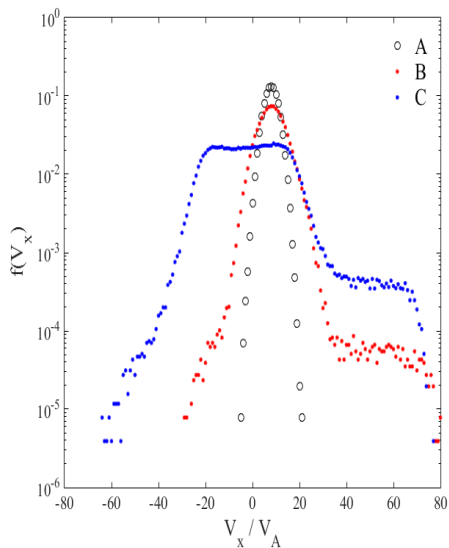
Simulation reproduces many observed features

Velocity distribution function:
A. Initial stage (black circle),
B. Early stage (red dot),
C. Later stage (blue dot).

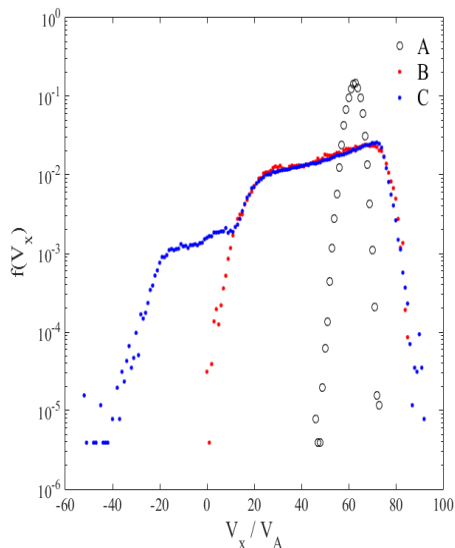


Time-evolution of
 wave energy δE_x^2

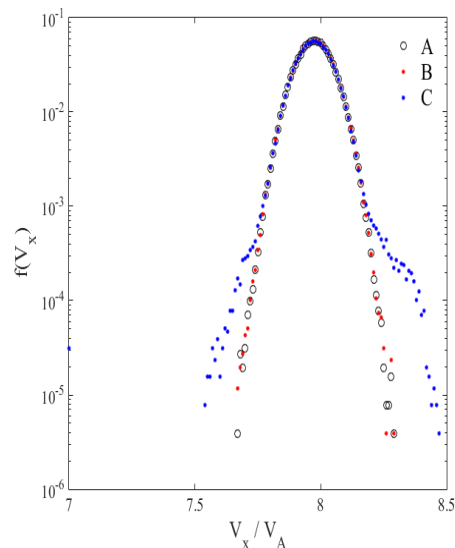
(a) Incident electrons



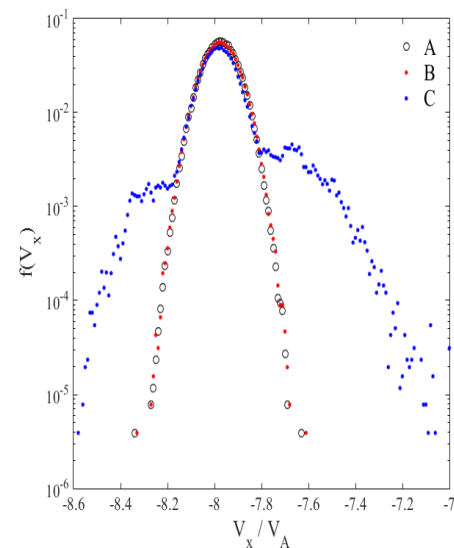
(b) Strahl electrons



(c) Incident ions



(d) Reflected ions



A Picture that is forming,

- Field-aligned currents produced by strahl electrons drifting SW core electrons are unstable (Very spontaneous)
- This instability produces large-amplitude ES waves.
- Later, the strahl phase space holes affect the reflected ions forming ion phase space holes.
- The ES waves heat plasma to temperature $>10^7$ °K, causing plasma to expand (in our case at super-Alfvénic speeds).
- Expansion reduces local plasma density and the edges steepen into shock waves.

The End

Questions about the Upstream nonlinear structures still not understood well.

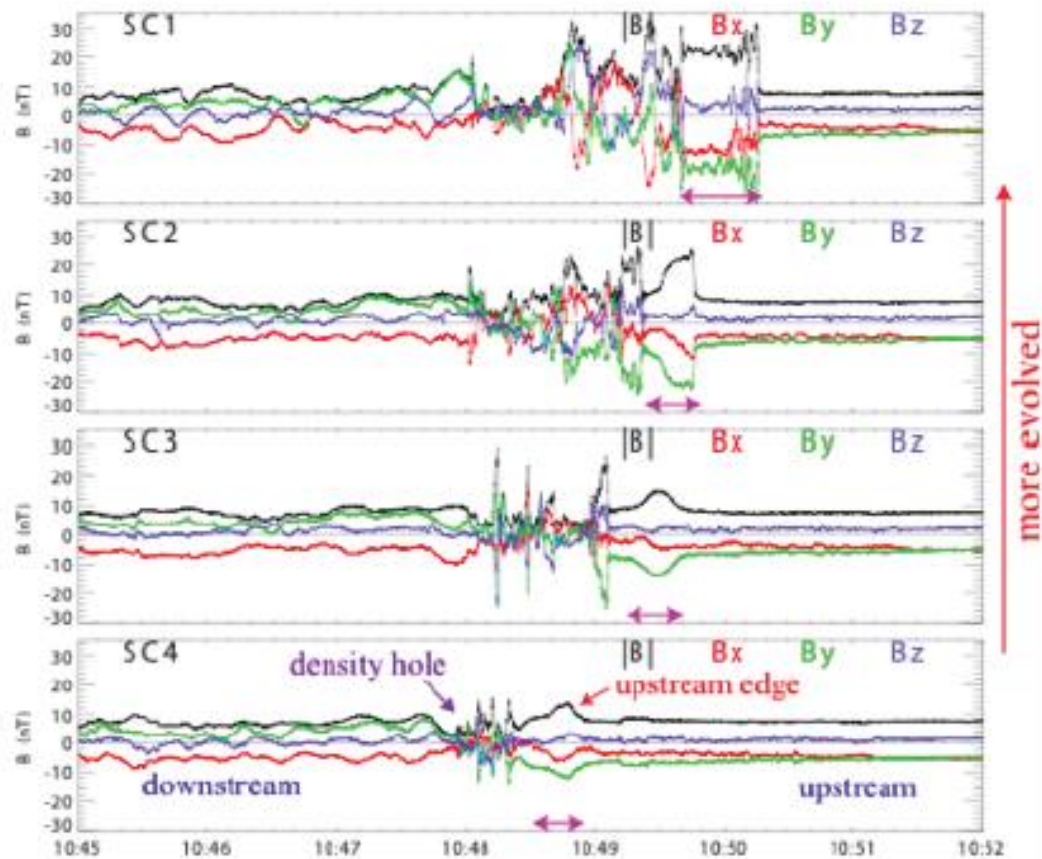
- What plasma processes can

(1) select an upstream wave to grow while the neighboring waves remain unchanged?

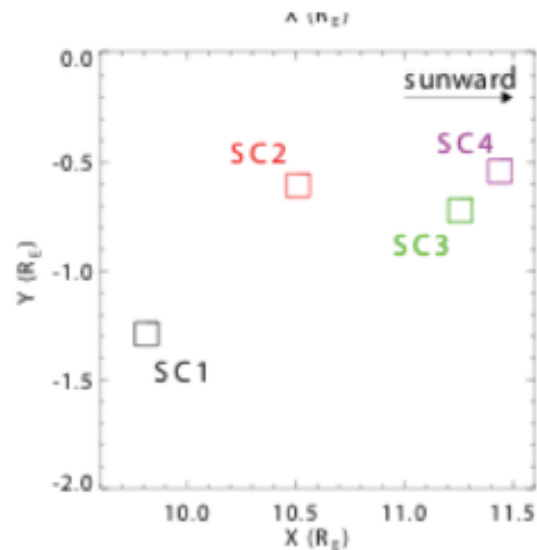
(2) evolve the magnetic pulsation into a complex nonlinear structure?

- Suggestion is that high temperature magnetosheath plasma comes from *reflected SW*.
- *Reflected SW* occupies a larger velocity space. Hence, temperature computed from second velocity moment is higher.
- But this is *not* a “heating” mechanism.
- Transmitted SW ions eventually isotropize as they move further away from the bow shock. Suggested mechanisms include cyclotron wave-particle interaction.
- Another possible source of Magsheath particles: Leakage of magnetospheric plasmas into the magnetosheath (Thomsen, 1983). O⁺ ions have been observed in the magnetosheath (Marcucci et al., 2000).

Magnetic field measurements (FGM) on Feb. 16, 2003



□ Evolution sequence : SC4 → SC3 → SC2 → SC1



Lee et al., 2009

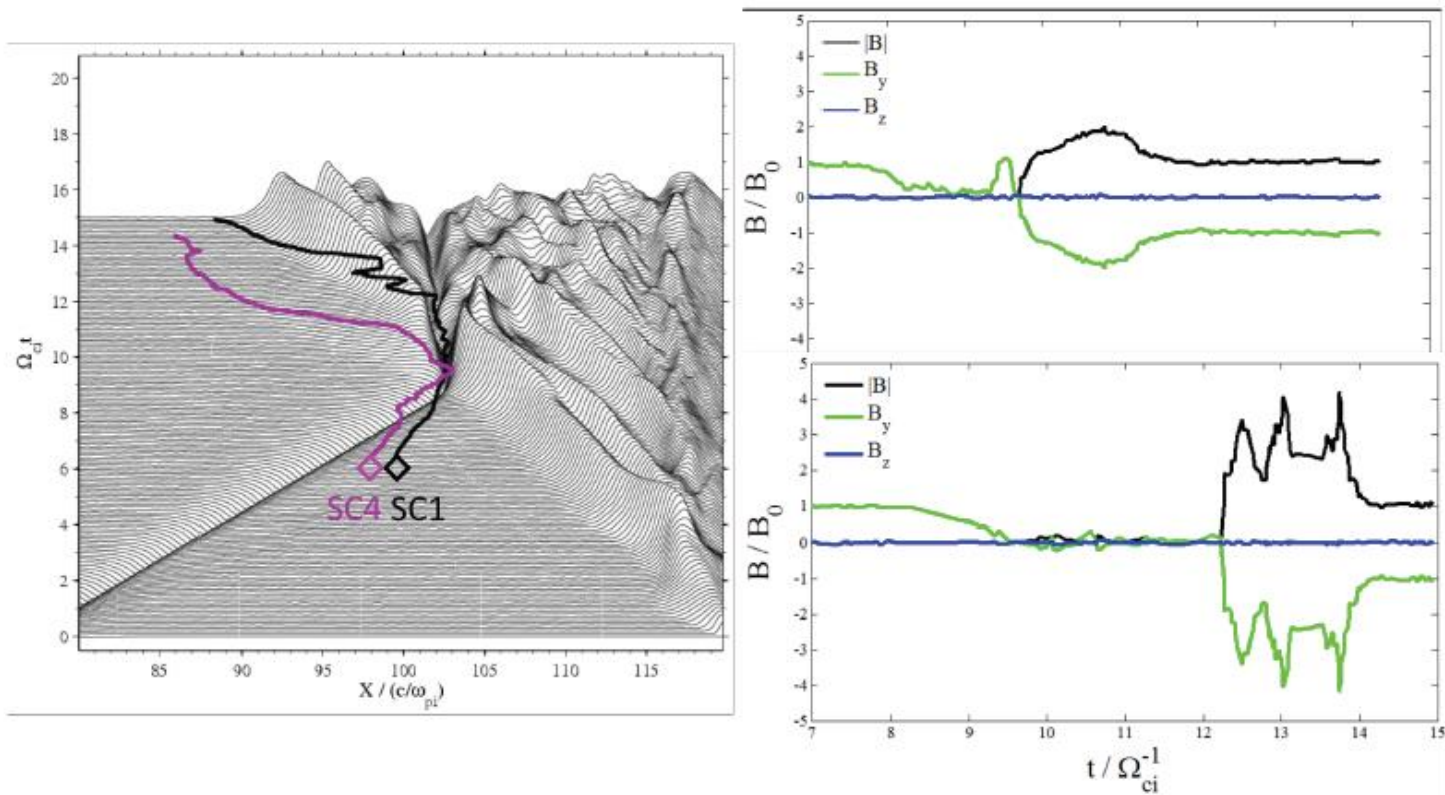
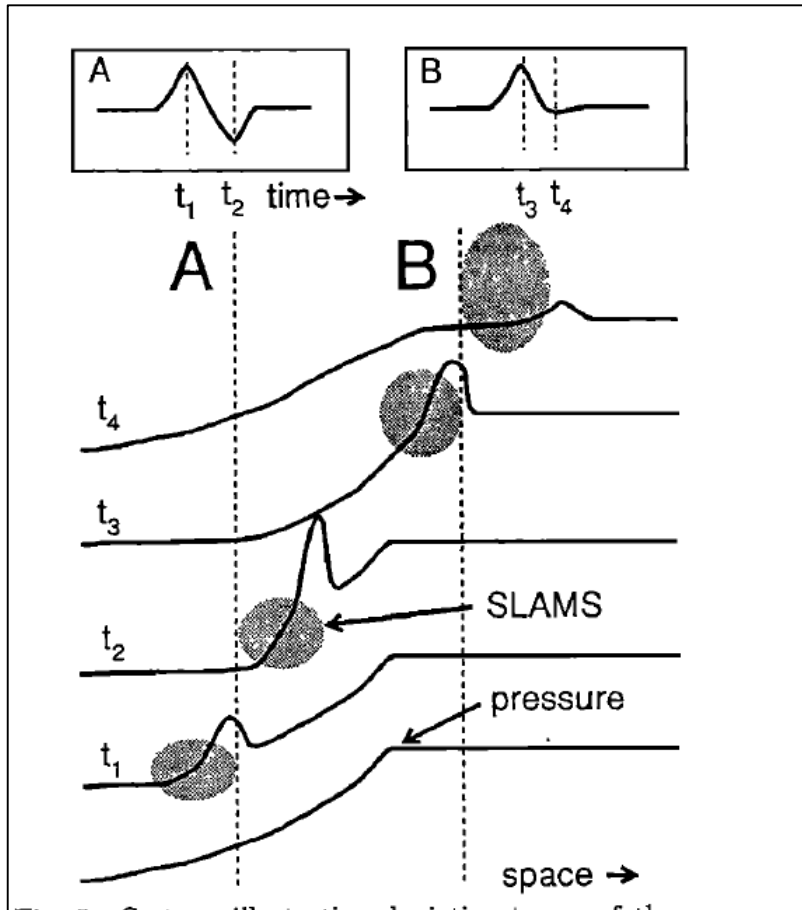


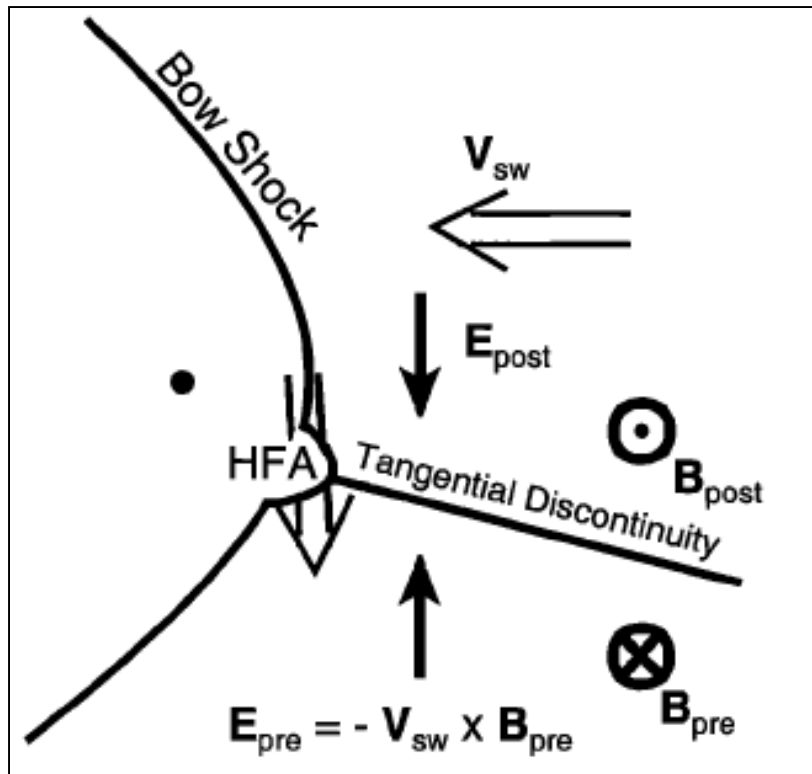
Figure 12: Simulation of an IMF current sheet interaction with the bow shock, originally suggested by Burgess and Schwartz (1988). The left panel shows the simulation results and the right the behavior of magnetic field measured by SC 1 and 4. For this simulation, we assumed that the leading edge of DH (Figure 9) develops into a perpendicular shock. The shock parameters used are ($\theta_{\text{Bn}}=90^\circ$, $M_A=4.5$, $\beta_i=1$, $\beta_e=0.5$).

Qualitative SLAMS Model



SLAMS due to *steepening of ULF wave* as it passes through energetic particle pressure gradient (Giacalone, 1993).

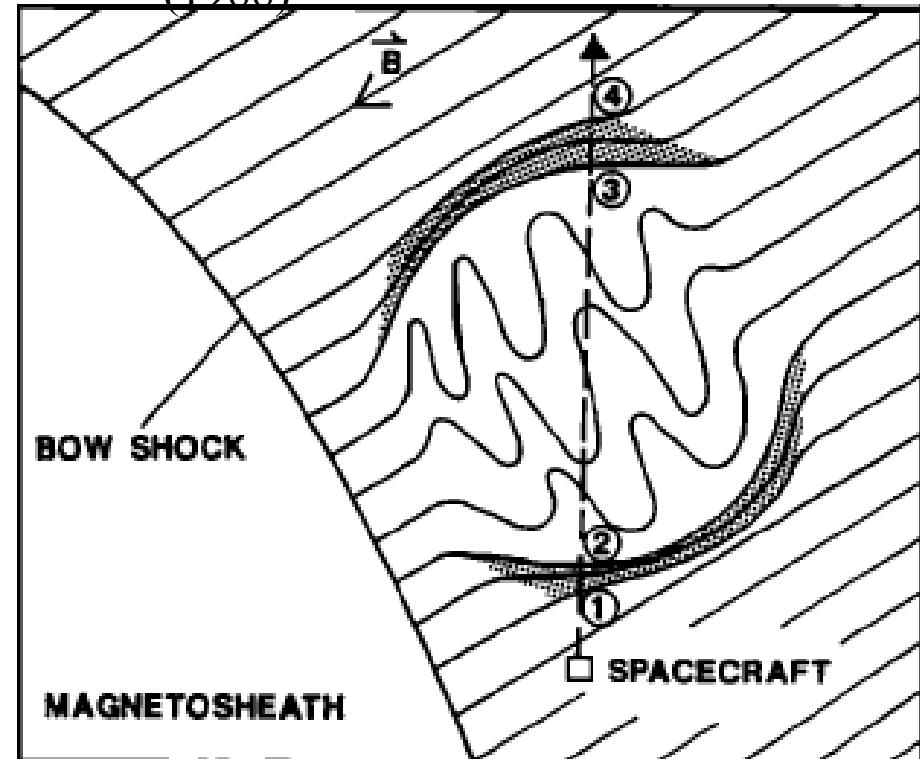
HFA Model: Burgess and Schwartz (1988)



- HFA associated passage of *IMF current sheet* (CS).
- SW E-field points *inward* normal to CS.
- Channels the *reflected particles* into the CS producing a high T region.
- Hot plasma expands
- No Instability involved.

HDC model: Thomsen et al.

(1988)



- HDCs due to *large fraction of reflected particles* coupled to SW
- *Ion-ion streaming instability* converts streaming energy to thermal energy
- Hot plasma expands
- Only Ion Dynamics

